Synthesis of $[(Me_3SiNCH_2CH_2)_3N]^{3-}$ and $[(C_6F_5NCH_2CH_2)_3N]^{3-}$ Complexes of Molybdenum and Tungsten That Contain CO, Isocyanides, or Ethylene

George E. Greco, Myra B. O'Donoghue, Scott W. Seidel, William M. Davis, and Richard R. Schrock*

Department of Chemistry 6-331, Massachusetts Institute of Technology, Cambridge, Massachusetts 02139

Received September 23, 1999

Paramagnetic complexes of the type $[N_3N]MoL$ ($[N_3N]^{3-} = [(Me_3SiNCH_2CH_2)_3N]^{3-}$; L = CO, RNC, C_2H_4) have been prepared by displacing dinitrogen from $[N_3N]Mo(N_2)$. $[N_3N]Mo(CO)$ was reduced by magnesium powder in the presence of Me_3SiCl to yield the diamagnetic oxycarbyne complex $[N_3N]Mo{\equiv}COSiMe_3$, while oxidation of $[N_3N]Mo(CN\text{-}t\text{-}Bu)$ with $[Cp_2Fe]OTf$ yielded $\{[N_3N]Mo(CN\text{-}t\text{-}Bu)\}OTf$. Thermolysis of $[N_3N]Mo(CN\text{-}t\text{-}Bu)$ resulted in loss of a t-Bu radical to yield $[N_3N]Mo(CN)$, which was structurally characterized. $[N_3N_F]ML$ ($[N_3N_F]^{3-} = [(C_6F_5NCH_2CH_2)_3N]^{3-}$; M = Mo, W; L = CO, RNC) complexes have been prepared by one-electron reduction of $[N_3N_F]M(OTf)$ in the presence of L. An X-ray study of $[N_3N_F]W(CN\text{-}t\text{-}Bu)$ showed it to contain a bent isocyanide ligand. Anionic CO complexes were prepared by the two-electron reduction of $[N_3N_F]M(OTf)$ in the presence of CO. An X-ray study of $\{[N_3N_F]W(CO)_2\}Na(ether)_3$ revealed it to have a pseudo-octahedral structure in which sodium is bound to the CO trans to the amine donor atom. Treatment of $\{[N_3N_F]M(CO)\}^-$ complexes with Me_3SiCl gave oxycarbyne complexes $[N_3N_F]M{\equiv}COSiMe_3$. Reaction of $[N_3N_F]WCO$ with $V(Mes)_3(THF)$ yielded $[N_3N_F]W(CO)V(Mes)_3$, the structure of which was determined in an X-ray study. Cationic $[N_3N_F]^{3-}$ complexes could be prepared that contain up to 3 equiv of isocyanide. An X-ray study of $\{[N_3N_F]W(CN\text{-}t\text{-}Bu)_3\}BPh_4$ showed it to be a seven-coordinate species with one isocyanide located in the equatorial plane and the other two isocyanide ligands in the apical pocket. Reduction of $[N_3N_F]W(OTf)$ under ethylene gave $[N_3N_F]W(C_2H_4)$, which could be oxidized to yield diamagnetic $\{[N_3N_F]W(C_2H_4)\}OTf$.

Introduction

In the last several years a wide variety of transition-metal complexes that contain a triamidoamine ligand, $[(RNCH_2CH_2)_3N]^{3-}$ (R = C_6F_5,[1,2] $SiMe_3$[3−9]), have been synthesized in our laboratories;[10] recently we have been able to extend this series to ligands in which R is an ordinary aryl group.[11] The salient features of such complexes are the sterically protected, 3-fold-symmetric, apical coordination site and the spatial arrangement of three metal bonding orbitals (two π and one σ) within this pocket. The relatively well-protected nature of the apical coordination site in $[N_3N]^{3-}$ ($[N_3N]^{3-} = [(Me_3SiNCH_2CH_2)_3N]^{3-}$) complexes in particular has allowed us to isolate unusual complexes such as trigonal-monopyramidal complexes that contain the first-row metals from titanium to iron,[12] a tantalum phosphinidene complex,[13] and tungsten and molybdenum terminal phosphido and arsenido complexes.[4] The presence of one σ and two π orbitals is ideal for the formation of $[N_3N]M{\equiv}E$ complexes (M = Mo, W; E = CR, N, P, As).[4] Alternatively, the metal center can bind two ligands via a single and a double bond, as in the alkylidene hydride complex $[N_3N]W(C_5H_8)(H)$.[8,9] The third bonding mode in which the metal forms single bonds to three ligands is uncommon, in part for steric reasons, with $[N_3N]WH_3$[9,14] being a rare example. Three-coordinate molybdenum triamido complexes are related to triamidoamine complexes, although they are unique in some respects, such as their ability to cleave dinitrogen homolytically to yield Mo(VI) nitrido species.[15,16]

(1) Kol, M.; Schrock, R. R.; Kempe, R.; Davis, W. M. *J. Am. Chem. Soc.* **1994**, *116*, 4382.
(2) Seidel, S. W.; Schrock, R. R.; Davis, W. M. *Organometallics* **1998**, *17*, 1058.
(3) Verkade, J. G. *Acc. Chem. Res.* **1993**, *26*, 483.
(4) Mösch-Zanetti, N. C.; Schrock, R. R.; Davis, W. M.; Wanninger, K.; Seidel, S. W.; O'Donoghue, M. B. *J. Am. Chem. Soc.* **1997**, *119*, 11037.
(5) Schrock, R. R.; Seidel, S. W.; Mösch-Zanetti, N. C.; Shih, K.-Y.; O'Donoghue, M. B.; Davis, W. M.; Reiff, W. M. *J. Am. Chem. Soc.* **1997**, *119*, 11876.
(6) O'Donoghue, M. B.; Davis, W. M.; Schrock, R. R. *Inorg. Chem.* **1998**, *37*, 5149.
(7) O'Donoghue, M. B.; Davis, W. M.; Schrock, R. R.; Reiff, W. M. *Inorg. Chem.* **1999**, *38*, 243.
(8) Schrock, R. R.; Seidel, S. W.; Mösch-Zanetti, N. C.; Dobbs, D. A.; Shih, K.-Y.; Davis, W. M. *Organometallics* **1997**, *16*, 5195.
(9) Schrock, R. R.; Shih, K.-Y.; Dobbs, D.; Davis, W. M. *J. Am. Chem. Soc.* **1995**, *117*, 6609.
(10) Schrock, R. R. *Acc. Chem. Res.* **1997**, *30*, 9.
(11) Greco, G. E.; Popa, A. I.; Schrock, R. R. *Organometallics* **1998**, *17*, 5591.
(12) Cummins, C. C.; Lee, J.; Schrock, R. R.; Davis, W. M. *Angew. Chem., Int. Ed. Engl.* **1992**, *31*, 1501.
(13) Cummins, C. C.; Schrock, R. R.; Davis, W. M. *Angew. Chem.* **1993**, *115*, 758.
(14) Dobbs, D. A.; Schrock, R. R.; Davis, W. M. *Inorg. Chim. Acta* **1997**, *263*, 171.
(15) Cummins, C. C. *Prog. Inorg. Chem.* **1998**, *47*, 685−836.

10.1021/om990748u CCC: $19.00
Publication on Web 02/17/2000

Scheme 1

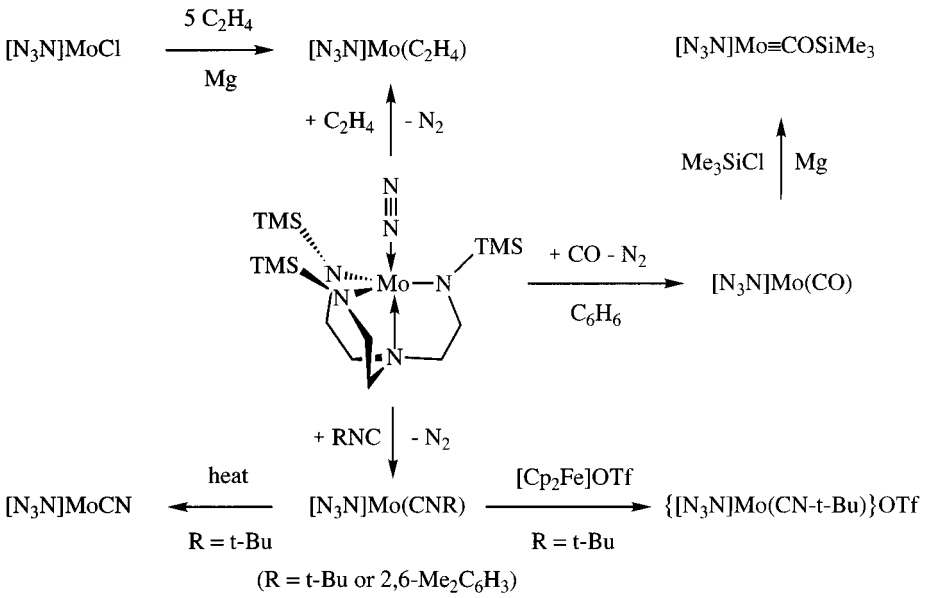

One of the original goals of the chemistry of transition-metal triamidoamine complexes was to understand how dinitrogen might be activated and reduced in a C_3-symmetric environment.[1,6,7] We now know that $\{[N_3N]Mo(N_2)\}^-$ can be formed readily upon reduction of $[N_3N]MoCl$ with excess magnesium and that it can be oxidized to form $[N_3N]Mo(N_2)$.[6,7] $\{[N_3N_F]Mo(N_2)\}^-$ ($[N_3N_F]^{3-} = [(C_6F_5NCH_2CH_2)_3N]^{3-}$) also can be formed readily, although $[N_3N_F]Mo(N_2)$ is still unknown. One could argue that as far as binding dinitrogen and related ligands is concerned, the $[N_3N]Mo$ and $[N_3N_F]W$ platforms might be approximately the same, the greater reducing power of W(III) versus Mo(III) being attenuated by the electron-withdrawing ability of the C_6F_5 groups. However, reduction of $[N_3N_F]W(OTf)$ or $[N_3N_F]WCl$ under dinitrogen so far has not yielded any dinitrogen complexes. Therefore, we became interested in comparing examples of $[N_3N]Mo$ and $[N_3N_F]M$ (M = Mo, W) complexes that contain other π back-bonding ligands such as CO, RNC, and ethylene. This type of organometallic chemistry would be different from that explored so far, which has been dominated by alkyl, alkylidene, and alkylidyne complexes of Mo(IV) or W(IV),[2,5] and more relevant to activation and reduction of dinitrogen. In this paper we report the synthesis of $[N_3N]Mo$ or $[N_3N_F]M$ (M = Mo, W) complexes that contain CO, isonitriles, and ethylene. The chemistry of $[N_3N]W$ complexes is limited by the low-yield synthesis of $[N_3N]WCl$;[8] therefore, similar $[N_3N]W$ chemistry was not explored.

Results

Synthesis and Reactivity of $[N_3N]Mo$ Complexes. Attempts to synthesize $[N_3N]Mo(CO)$ in THF by reducing $[N_3N]MoCl$ with magnesium powder in the presence of 1 equiv of CO failed; $[N_3N]MoCl$ was recovered unchanged. However, $[N_3N]Mo(CO)$ could be accessed by substituting dinitrogen in $[N_3N]Mo(N_2)$ with CO (Scheme 1). Exposure of benzene solutions of $[N_3N]Mo(N_2)$ to 1 equiv of CO resulted in a color change from orange to emerald green over the course of 15 min; $[N_3N]Mo(CO)$ could be isolated from the reaction as green needles in 85% yield. When an excess of CO was used in this reaction, a mixture of $[N_3N]Mo(CO)$ and $[N_3N]Mo{\equiv}COSiMe_3$ (see below) was formed, along with other decomposition products. The ^1H NMR spectrum of $[N_3N]Mo(CO)$ consists of two broad resonances at 13.17 and −38.04 ppm for the methylene protons in the $[N_3N]^{3-}$ backbone (Table 1) and a sharper resonance at −2.03 ppm, which we assign to the $SiMe_3$ groups. This spectrum is similar to the ^1H NMR spectrum of $[N_3N]Mo(N_2)$[6] and other $[N_3N]Mo(L)$ complexes reported here, in that one of the backbone methylene resonances is found downfield of the TMS resonance. In $[N_3N]MoCl$ and other paramagnetic d^2 complexes,[10] including those reported here (Table 1), both backbone methylene resonances are found upfield of 0 ppm.[10]

The IR spectrum of $[N_3N]Mo(CO)$ in pentane has a strong, sharp CO stretch at 1859 cm^{-1}, which lies toward the low end of the range of typical stretching frequencies for neutral, terminal CO complexes.[17] The *two* peaks found in the IR spectrum of $[N_3N]Mo(CO)$ in Nujol at 1841 and 1832 cm^{-1} we believe can be attributed to the presence of two molecules in the unit cell, a circumstance that also gave rise to two peaks in the solid-state (Nujol) IR spectrum of $[N_3N]Mo(N_2)$, but one in solution.[6] SQUID magnetic susceptibility data for solid $[N_3N]Mo(CO)$ over the temperature range 5−300 K could be fit to the Curie law to give $\mu = 1.74(1)\ \mu_B$ ($R = 0.9998$), a value that is close to the spin-only moment for a system containing one unpaired electron. When a C_6D_6 solution of $[N_3N]Mo(CO)$ was heated to 80 °C for 1 week, the color darkened slightly and ^1H NMR spectra revealed that ∼10% $[N_3N]Mo{\equiv}COSiMe_3$ (see below) was present, along with other unidentified decomposition products.

(16) Peters, J. C.; Cherry, J.-P.; Thomas, J. C.; Baraldo, L.; Mindiola, D. J.; Davis, W. M.; Cummins, C. C. *J. Am. Chem. Soc.* **1999**, *121*, 10053.

(17) Collman, J. P.; Hegedus, L. S.; Norton, J. R.; Finke, R. G. *Principles and Applications of Organotransition Metal Chemistry*, 2nd ed.; University Science Books: Mill Valley, CA, 1987.

Table 1. IR, Magnetic, and Selected NMR Data for CO, Isocyanide, and Ethylene Complexes[a]

compd	IR[b] (cm^{-1})	magnetism[c] (μ_B)	ligand CH_2 NMR (ppm)	
$[N_3N]Mo(CO)$	1859 (pentane) 1841, 1832 (N)	1.74 (S)	13.2	−38.0
$[N_3N]Mo(CN\text{-}t\text{-}Bu)$	1838 (N)	1.74 (S)	13.4	−39.0
$[N_3N]Mo(CNAr)$	1740 (N)	P	61.9	−29.8
$\{[N_3N]Mo(CN\text{-}t\text{-}Bu)\}OTf$	2147 (THF)	2.71 (S)	−29.4	−98.1
$[N_3N]Mo(CN)$	not obsd	2.73 (S)	−25.7	−112.4
$[N_3N]Mo(C_2H_4)$		1.73 (S)	not obsd	
$[N_3N_F]Mo(CO)$	1889 (N)	2.1 (E)	12.9	−23.9
$\{[N_3N_F]Mo(CO)\}Na(15\text{-crown-}5)$	1695 (N)	D	3.73	2.22
$[N_3N_F]W(CO)$	1846 (N)	2.6 (E)	29.3	−19.2
$\{[N_3N_F]W(CO)\}Na(15\text{-crown-}5)$	1628 (N)	D	3.63	2.20
$[N_3N_F]Mo(CN\text{-}t\text{-}Bu)$	1787 (N)	2.4 (E)	6.6	−28.2
$[N_3N_F]Mo(CNAr)$	1777 (N)	2.2 (E)	26.2	−22.7
$[N_3N_F]Mo(CN\text{-}n\text{-}Bu)$	1790 (N)	2.3 (E)	5.7	−27.6
$[N_3N_F]W(CN\text{-}t\text{-}Bu)$	1684 (N)	1.74 (S), 2.2 (E)	8.0	−25.8
$[N_3N_F]W(CNAr)$	1679 (N)	2.2 (E)	31.8	−25.1
$\{[N_3N_F]W(CN\text{-}t\text{-}Bu)\}BAr^F{}_4$	2136 (N)	2.8 (E)	−28.1	−55.0
$\{[N_3N_F]W(CNAr)\}BAr^F{}_4$	2066 (N)	2.8 (E)	−27.8	−55.2
$\{[N_3N_F]Mo(CN\text{-}t\text{-}Bu)\}BAr^F{}_4$	2184 (N)	3.1 (E)	−20.2	−80.7
$\{[N_3N_F]Mo(CNAr)\}BAr^F{}_4$	2133 (N)	3.3 (E)	−21.0	−81.2
$\{[N_3N_F]W(CN\text{-}t\text{-}Bu)_2\}OTf$	2111, 2104 (N)	D	4.09	3.76
$\{[N_3N_F]W(CNAr)_2\}OTf$	2096, 2058 (N)	D	4.18	3.92
$[N_3N_F]Mo(CN\text{-}t\text{-}Bu)_2OTf$	2162, 2136 (N)	D	4.06	3.65
$[N_3N_F]Mo(CNAr)_2OTf$	2116, 2095 (N)	D	4.28	3.97
$[N_3N_F]W(CN\text{-}t\text{-}Bu)_3OTf$	2178, 2145 (N)	D	complex mutiplet	
$[N_3N_F]W(C_2H_4)$		1.8 (E)	not obsd	
$\{[N_3N_F]W(C_2H_4)\}OTf$		D	4.42	3.96

[a] IR: free ArNC, 2115 cm^{-1}; t-BuNC, 2136 cm^{-1}; CO, 2143 cm^{-1}. [b] Legend: N = Nujol. [c] Legend: S = SQUID; E = Evans method; D = diamagnetic; p = paramagnetic.

When THF solutions of $[N_3N]Mo(CO)$ are stirred over magnesium powder in the presence of Me_3SiCl, the color changes from deep green to yellow over the course of 15 min. Diamagnetic $[N_3N]Mo{\equiv}COSiMe_3$ can be isolated from the reaction as pale yellow needles in 91% yield (Scheme 1). In the absence of Me_3SiCl, two diamagnetic complexes are observed by ^1H NMR spectroscopy that have characteristic resonances for a diamagnetic $[N_3N]^{3-}$ complex. They are tentatively formulated as $\{[N_3N]Mo(CO)\}_2Mg(THF)_2$ and $\{[N_3N]Mo(CO)\}MgCl(THF)_2$, the CO analogues of $\{[N_3N]Mo(N_2)\}_2Mg(THF)_2$ and $\{[N_3N]Mo(N_2)\}MgCl(THF)_2$,[6] respectively. No attempt was made to isolate these complexes. They react immediately with Me_3SiCl to give $[N_3N]Mo{\equiv}COSiMe_3$, according to NMR studies. The ^1H NMR spectrum of $[N_3N]Mo{\equiv}COSiMe_3$ consists of two TMS resonances in the ratio of 3:1 and a pair of triplets for the methylene protons on the ligand backbone. In the ^{13}C NMR spectrum of $[N_3N]Mo{\equiv}COSiMe_3$ the alkylidyne carbon resonance is found at 208.3 ppm, a chemical shift that is approximately 90 ppm to higher field than typically found for alkylidyne complexes of this type that contain a proton or a carbon substituent.[2,5] No CO stretch could be identified in the IR spectrum in Nujol.

No reaction is observed between $[N_3N]MoCl$ and magnesium powder in the presence of 1 equiv of t-BuNC. Paramagnetic $[N_3N]Mo(CN\text{-}t\text{-}Bu)$ can be isolated in a reaction in which $[N_3N]MoCl$ is reduced by Na/Hg amalgam in the presence of t-BuNC, but the reaction is not clean and $[N_3N]Mo(CN\text{-}t\text{-}Bu)$ is contaminated with $[N_3N]MoCl$. A clean, high-yield route to $[N_3N]Mo(CN\text{-}t\text{-}Bu)$ consists of the reaction between $[N_3N]Mo(N_2)$ and t-BuNC (Scheme 1). Upon addition of t-BuNC to a toluene solution of $[N_3N]Mo(N_2)$ the color changes to deep orange and $[N_3N]Mo(CN\text{-}t\text{-}Bu)$ can be isolated as rust-colored needles in 96% yield. The IR, magnetic, and NMR data listed in Table 1 suggest that low-spin $[N_3N]Mo(CN\text{-}t\text{-}Bu)$ is a close relative of $[N_3N]Mo(CO)$. $[N_3N]Mo(CNAr)$ (Ar = 2,6-dimethylphenyl) can be prepared in an analogous manner.

Ferrocenium triflate reacts smoothly with $[N_3N]Mo(CN\text{-}t\text{-}Bu)$ in THF to give $\{[N_3N]Mo(CN\text{-}t\text{-}Bu)\}OTf$ quantitatively as an orange powder. In the ^1H NMR spectrum of $\{[N_3N]Mo(CN\text{-}t\text{-}Bu)\}OTf$ the resonances for the methylene protons of the ligand backbone are both found upfield of the resonance attributed to the TMS groups of the ligand at 12.83 ppm (Table 1), which is typical of paramagnetic d^2 $[N_3N]Mo$ complexes. The higher CN stretching frequency in $\{[N_3N]Mo(CN\text{-}t\text{-}Bu)\}OTf$ in THF (2147 cm^{-1}) reflects the weak π backbonding from the cationic d^2 metal center compared to that of the d^3 metal center in $[N_3N]Mo(CN\text{-}t\text{-}Bu)$ (1838 cm^{-1}). The proposed high-spin d^2 configuration of $\{[N_3N]Mo(CN\text{-}t\text{-}Bu)\}OTf$ is further supported by SQUID magnetic susceptibility measurements over the temperature range 5−300 K, which reveal a behavior analogous to that observed for $[N_3N]MoMe$ and $[N_3N]MoCl$ (χ approaches a constant as T approaches 0 K)[5] and which we now assume to be characteristic of paramagnetic d^2 $[N_3N]Mo$ complexes of this general type (Figure 1). The data can be fit to a Curie−Weiss law ($\chi = \mu^2/8(T - \Theta)$) over the temperature range 30−300 K to yield a value of $\mu = 2.71(4)\ \mu_B$ and $\Theta = -5(1)$ K, consistent with two unpaired electrons being present, presumably in the d_{xz} and d_{yz} orbitals. This type of behavior has been attributed[5] to a combination of spin−orbit coupling and low-symmetry ligand field components that result in zero-field splitting of the d^2 ground-state spin triplet.[18]

$[N_3N]Mo(CN\text{-}t\text{-}Bu)$ proved to be thermally unstable. When a toluene solution of $[N_3N]Mo(CN\text{-}t\text{-}Bu)$ was heated to 86 °C for 36 h, the color changed from orange

(18) Figgis, B. N.; Lewis, J. *Prog. Inorg. Chem.* **1964**, *6*, 37.

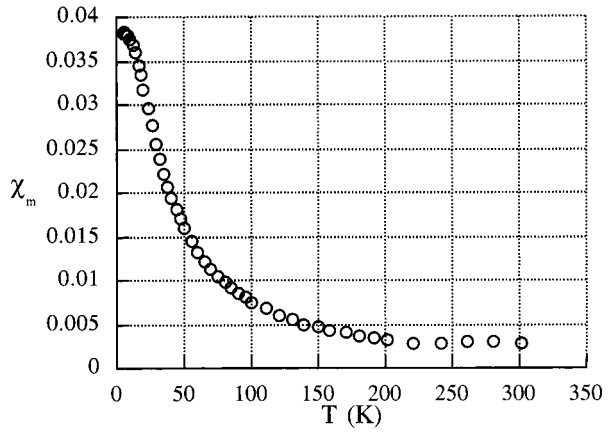

Figure 1. Plot of χ_m (corrected for diamagnetism using Pascal's constants) versus *T* for {[N_3N]Mo(CN-t-Bu)}OTf.

to yellow. When the thermolysis was carried out in C_6D_6 in a sealed NMR tube, ^{1}H NMR spectra of the crude reaction mixture revealed three broad, paramagnetically shifted resonances at 7.73, −25.7, and −112.4 ppm, characteristic of a new C_3-symmetric complex. Resonances were also observed for isobutylene, isobutane, and hexamethylethane, products that we propose arise from the disproportionation and coupling of t-Bu radicals. Yellow, crystalline [N_3N]Mo(CN) could be isolated from the thermolysis reaction in 88% yield (Scheme 1). A plot of the molar magnetic susceptibility of [N_3N]Mo(CN) versus temperature is characteristic of paramagnetic d^2 [N_3N]MoX complexes of this general type. The data can be fit to the Curie−Weiss law over the temperature range 30−300 K to give $\mu = 2.73(1)\ \mu_B$ and $\Theta = -7.1(3)$ K. A CN stretch could not be located in the IR spectrum of [N_3N]Mo(CN). (The IR spectrum of the analogous tungsten complex[19] also lacks an absorption that could be assigned to the cyanide ligand.)

Single crystals of [N_3N]Mo(CN) were grown from a saturated diethyl ether solution at −30 °C and examined in an X-ray study. Crystallographic data and collection and refinement parameters are given in Table 2. The molecular structure of [N_3N]Mo(CN) is shown in Figure 2, while selected bond lengths, bond angles, and dihedral angles are listed in Table 3. The structure of [N_3N]Mo(CN) bears a striking resemblance to that of [N_3N]MoCl.[20] The Mo−N_{amide} bond distances are statistically identical in the two complexes, as are the Mo−N_{ax} bond distances. The TMS groups also are all oriented upright in both complexes, as measured by N_{ax}−Mo−N_{eq}−Si dihedral angles close to 180°, indicative of little steric pressure within the pocket. For comparison, in [N_3N]Mo(OTf) the dihedral angles range from 136 to 143°, since the TMS groups twist in response to the sterically bulky triflate ligand within the pocket.[5]

Unlike [N_3N]Mo(CN-t-Bu), [N_3N]Mo(CNAr) showed no evidence of decomposition after a solution had been heated to 80 °C for 12 h. The greater stability of aryl isocyanides compared to that of *tert*-butyl isocyanide toward decomposition via homolytic N−C bond cleavage is to be expected. For example, *trans*-Mo(PhNC)$_2$(Me$_8$[16]aneS_4) is also relatively stable toward decomposition to yield *trans*-Mo(CN)$_2$(Me$_8$[16]aneS_4).[21]

Reduction of [N_3N]MoCl in THF with an excess of magnesium powder in the presence of 5 equiv of ethylene proceeds smoothly over a period of 12 h to give a purple solution that contains paramagnetic [N_3N]Mo(C_2H_4) (Scheme 1). The ethylene complex can be isolated as purple needles in 97% yield upon recrystallization from hexamethyldisiloxane. Exposing C_6D_6 solutions of orange [N_3N]Mo(N_2) to excess ethylene (10 equiv) also yielded [N_3N]Mo(C_2H_4) rapidly and cleanly according to ^{1}H NMR spectra. Unlike other Mo(III) adducts described so far, resonances for the methylene protons of the ligand backbone in [N_3N]Mo(C_2H_4) were not observed in its ^{1}H NMR spectrum; only a single broad resonance was observed at 3.63 ppm ($\Delta\nu_{1/2}$ = 414 Hz) that we assign to the TMS groups of the ligand. A resonance attributable to the ethylene ligand also could not be observed. Toluene-d_8 solutions of [N_3N]Mo(C_2H_4) show little change after being heated in vacuo at 60 °C for 14 h. However, after a sample was heated to 90 °C in toluene under 1 atm of dinitrogen for 1 week, the ^{1}H NMR spectrum revealed the presence of [N_3N]Mo−N=N−Mo[N_3N][6] and [N_3N]Mo(N_2), along with [N_3N]Mo(C_2H_4). Therefore, we presume that [N_3N]Mo(C_2H_4) and [N_3N]Mo(N_2) are in equilibrium with each other, although the breadth of the TMS resonance in the spectrum of [N_3N]Mo(C_2H_4) and its coincidental overlap with the TMS resonance in the spectrum of [N_3N]Mo−N=N−Mo[N_3N] precluded any accurate estimate of the extent of its conversion to the dinitrogen complexes. In any case the equilibrium would appear to be reached slowly. A SQUID study shows that the magnetic susceptibility of [N_3N]Mo(C_2H_4) obeys the Curie law between 5 and 300 K ($\mu = 1.73(1)\ \mu_B$ with $R = 0.9999$), consistent with [N_3N]Mo(C_2H_4) being a low-spin Mo(III) complex.

Oxidation of [N_3N]Mo(C_2H_4) by ferrocenium triflate gave [N_3N]Mo(OTf)[5] as the only identifiable product, according to ^{1}H NMR spectroscopy. Since ethylene is somewhat labile in [N_3N]Mo(C_2H_4), we assume that it is even more labile in hypothetical {[N_3N]Mo(C_2H_4)}$^+$ as a consequence of reduced back-bonding from the cationic d^2 metal center. Loss of ethylene folowed by triflate attack at the cationic Mo center then produces [N_3N]Mo(OTf). This behavior is in contrast with the result of oxidation of [N_3N_F]W(C_2H_4) with ferrocenium triflate to give {[N_3N_F]W(C_2H_4)}OTf (vide infra).

Synthesis and Reactivity of [N_3N_F]M (M = Mo, W) Carbonyl Complexes. Reduction of [N_3N_F]Mo(OTf) with 2 equiv of sodium amalgam in the presence of excess CO gives {[N_3N_F]Mo(CO)}Na(THF)$_x$ (Scheme 2). The amount of THF in the isolated compound varies from sample to sample (according to proton NMR spectra). Addition of 15-crown-5 to a THF solution of the crude product yields {[N_3N_F]Mo(CO)}Na(15-crown-5), which can be crystallized from a mixture of toluene and pentane at −40 °C. The proton, carbon, and fluorine NMR spectra of {[N_3N_F]Mo(CO)}Na(15-crown-5) are all consistent with a trigonally symmetric diamagnetic species. The resonance for the carbonyl carbon is found at 226.7 ppm in the ^{13}C NMR spectrum. Since a CO

(19) Dobbs, D. A. Unpublished observations.
(20) Duan, Z.; Verkade, J. G. *Inorg. Chem.* **1995**, *34*, 1576.
(21) Adachi, T.; Nobuyoshi, S.; Ueda, T.; Kaminaka, M.; Yoshida, T. *J. Chem. Soc., Chem. Commun.* **1989**, 1320.

Table 2. Crystallographic Data, Collection Parameters, and Refinement Parameters for [N_3N]Mo(CN), [N_3N_F]W(CO)V(Mes)$_3$, and [N_3N_F]W(CN-t-Bu)[a]

	[N_3N]Mo(CN)	[N_3N_F]W(CO)V(Mes)$_3$	[N_3N_F]W(CN-t-Bu)
empirical formula	$C_{18}H_{44}N_5O_{0.50}Si_3Mo$	$C_{59}H_{52}F_{15}N_4OVW$	$C_{29}H_{21}F_{15}N_5W$
fw	518.79	1352.84	908.36
cryst dimens (mm)	0.37 × 0.32 × 0.23	0.12 × 0.12 × 0.10	0.21 × 0.14 × 0.08
cryst syst	tetragonal	monoclinic	monoclinic
a (Å)	16.5384(4)	12.1785(7)	9.344(4)
b (Å)	16.5384(4)	17.3080(10)	27.089(23)
c (Å)	9.8908(3)	26.374(2)	12.237(10)
β (deg)	90	95.6570(10)	97.26(5)
V (Å^3)	2705.32(12)	5532.2(5)	3072.8(37)
space group	$P\bar{4}2_1$	$P2_1/c$	$P2_1/c$
Z	4	4	4
D_{calcd} (Mg/m^3)	1.274	1.624	1.964
abs coeff (mm^{-1})	0.633	2.342	3.881
F_{000}	1100	2696	1756
temp (K)	183(2)	188 (2)	153(2)
θ range (deg)	1.74−23.23	1.41−20.00	1.50−23.32
no. of rflns collected	11 177	15 746	9917
no. of indep rflns	2052	5147	4215
R1 ($I > 2\sigma(I)$)[b]	0.0292	0.1078	0.0494
wR2 ($I > 2\sigma(I)$)[c]	0.0842	0.1955	0.1103
R1 (all data)	0.0320	0.1272	0.0555
wR2 (all data)	0.0929	0.2191	0.1141
GOF	0.936	1.400	1.216

[a] All structures were solved on a Siemens SMART/CCD diffractometer using 0.710 73 Å Mo Kα radiation. [b] $R1 = \sum||F_o| - |F_c||/\sum|F_o|$. [c] $wR2 = [(\sum w(|F_o| - |F_c|)^2/\sum wF_o^2)]^{1/2}$.

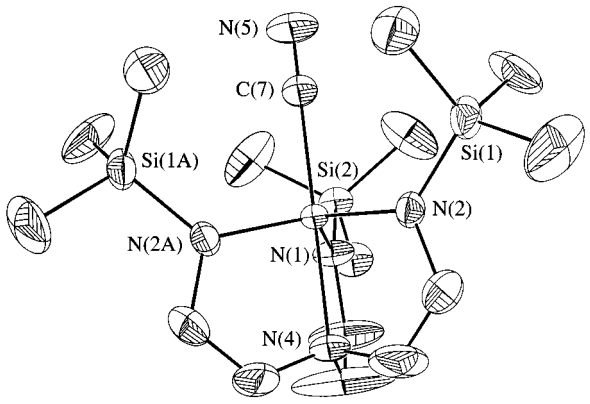

Figure 2. ORTEP drawing of [N_3N]Mo(CN).

Table 3. Selected Bond Lengths (Å) and Bond Angles (deg) for [N_3N]Mo(CN)

Bond Lengths (Å)			
Mo−N(1)	1.980(5)	Mo−C(7)	2.182(6)
Mo−N(2)	1.970(3)	C(7)−N(5)	1.113(8)
Mo−N(4)	2.210(5)		
Bond Angles (deg)			
Mo−N(2)−Si(1)	128.1(2)	N(1)−Mo−N(4)	80.9(2)
Mo−N(1)−Si(2)	128.3(3)	Mo−C(7)−N(5)	179.8(6)
N(2)−Mo-N(2A)	115.6(2)	C(7)−Mo-N(4)	179.1(2)
N(1)−Mo−N(2)	118.53(11)	N(2)−Mo−N(4)	80.92(12)
Dihedral Angles (deg)[a]			
N(4)−Mo−N(2)−Si(1)	179.1	N(4)−Mo−N(1)−Si(2)	180.0

[a] Obtained from a Chem 3D model.

stretch is observed at 1695 cm^{-1} in the IR spectrum in Nujol, sodium cannot be bound so strongly to oxygen as to justify a description of this species as an oxycarbyne derivative, i.e., [N_3N_F]Mo≡CONa(15-crown-5).

Addition of trimethylchlorosilane to {[N_3N_F]Mo(CO)}Na(THF)$_x$ results in immediate bleaching of the orange color and formation of what can be described as [N_3N_F]Mo≡COSiMe$_3$ (Scheme 2). The colorless product can be isolated in 50% yield by recrystallization from ether. The resonance for the carbonyl carbon is found at 212.4 ppm in the ^{13}C NMR spectrum, which is between values for the analogous [N_3N]Mo (208.3 ppm; vide supra) and [N_3N_F]W (214.1 ppm; vide infra) complexes.

Oxidation of {[N_3N_F]Mo(CO)}Na(15-crown-5) with 1 equiv of ferrocenium tetraphenylborate gives green, paramagnetic, [N_3N_F]Mo(CO) as the only metal-containing product (Scheme 2). Only two peaks are observed in the ^{19}F NMR spectrum of [N_3N_F]Mo(CO), and the proton NMR spectrum contains a high-field and a low-field resonance for the protons on the ligand backbone, consistent with what is found for the other neutral M(III) complexes in the present study. (The resonance for the ortho fluorine appears to be too broad to be located with confidence.) The CO absorption at 1889 cm^{-1} is at higher energy than in the analogous [N_3N]Mo complex (1845 cm^{-1}; vide supra) or the [N_3N_F]W complex (1846 cm^{-1}; vide infra), consistent with weaker back-bonding from the metal to CO in [N_3N_F]Mo(CO); i.e., the C_6F_5 ligand renders the metal more electron poor than the TMS ligand does, and W is a better reductant than Mo. A magnetic moment of 2.1 μ_B, which indicates one unpaired electron, was calculated from a magnetic susceptibility measurement in C_6D_6 solution using the Evans method. If {[N_3N_F]Mo(CO)}Na(15-crown-5) is oxidized with ferrocenium triflate, instead of ferrocenium tetraphenylborate, [N_3N_F]Mo(OTf) is the only compound that could be identified. We propose that it is produced by a two-electron oxidation of the metal and displacement of CO by triflate in the intermediate {[N_3N_F]Mo(CO)}OTf.

[N_3N_F]W(OTf) reacts with 1 equiv of 0.5% sodium amalgam under carbon monoxide to yield [N_3N_F]W(CO) as a paramagnetic red crystalline solid in high yield (Scheme 2). Only the meta and para fluorines can be observed in the ^{19}F NMR spectrum as broad resonances at −132.1 and −170.5 ppm. [N_3N_F]W(CO) is always contaminated with a *trace* (<5% by NMR) of a diamagnetic impurity, although the presence of this impurity

Scheme 2

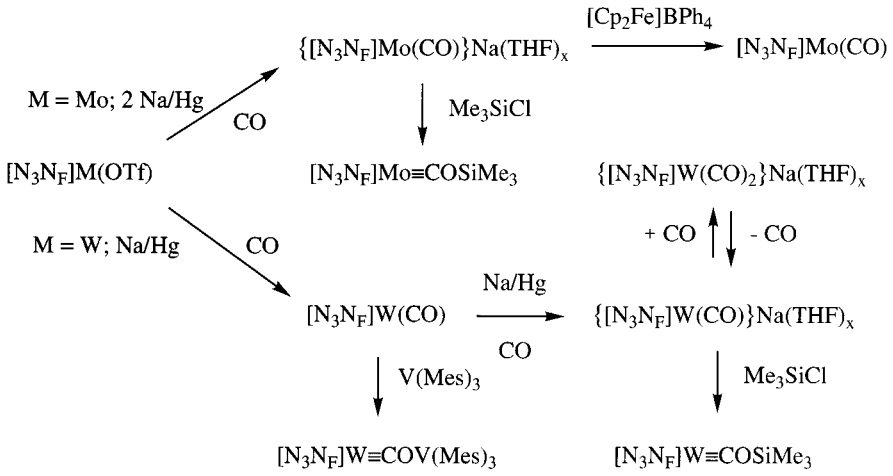

did not prevent successful C, H, and N analyses. A ^{13}C NMR study of the diamagnetic impurity present in a sample of $[N_3N_F]W(^{13}CO)$ revealed a sharp resonance at 205.1 ppm, which displayed tungsten satellite peaks (J_{CW} = 131 Hz). In the proton-coupled spectrum this peak splits into a doublet with J_{CH} = 7.5 Hz. Therefore, we propose that the diamagnetic impurity is either a carbonyl hydride complex, $[N_3N_F]W(CO)(H)$, analogous to crystallographically characterized $[N_3N]W(CO)(H)$, in which $\delta(C_\alpha)$ = 209 ppm and J_{CW} = 133 Hz,[8] or $[N_3N_F]W{\equiv}COH$, analogous to $[N_3N_F]W{\equiv}COSiMe_3$ described below, in which $\delta(C_\alpha)$ = 216.9 ppm. The origin of the hydrogen atom is not known. No reaction was observed when $[N_3N_F]WCl$ was stirred with Na/Hg under CO.

Reaction of $[N_3N_F]W(OTf)$ with 2 equiv of sodium amalgam in the presence of an excess of CO yields an intensely purple solution. When the solution is exposed to vacuum, the color changes to red and, ultimately, to yellow. Proton, carbon, and fluorine NMR spectra suggest that the yellow diamagnetic product is $\{[N_3N_F]W(CO)\}Na(THF)_x$, a stable crystalline derivative of which can be prepared by adding 15-crown-5 to it. The resonance for the carbonyl carbon occurs at 224.2 ppm (J_{CW} = 270 Hz) in the ^{13}C NMR spectrum of ^{13}C-labeled $\{[N_3N_F]W(CO)\}Na(15\text{-crown-}5)$ (cf. 226.7 ppm in $\{[N_3N_F]Mo(CO)\}Na(15\text{-crown-}5)$). The IR spectrum of $\{[N_3N_F]W(CO)\}Na(15\text{-crown-}5)$ contains a single CO stretching band at 1628 cm^{-1} (cf. 1695 cm^{-1} in the analogous Mo complex), which shifts to 1592 cm^{-1} in ^{13}C-labeled material, again consistent with the expected greater reducing power of tungsten compared to molybdenum.

We were interested in determining the identity of the purple material formed upon initial reduction of $[N_3N_F]W(OTf)$ in the presence of CO. The purple solution maintains its color indefinitely at room temperature in the presence of CO, or at −40 °C in the drybox freezer (under nitrogen). Since the anionic monocarbonyl complex can be isolated upon exposure of the purple solution to vacuum, we proposed that the purple material is $\{[N_3N_F]W(CO)_2\}Na(THF)_x$. This hypothesis is supported by the fact that exposing a solution of $\{[N_3N_F]W(CO)\}Na(THF)_x$ to CO (after removing dinitrogen from solution via the freeze−pump−thaw method) results in the reappearance of the purple color. The ^{19}F NMR spectrum shows a 2:1 ratio of all three types of fluorine in the molecule, consistent with the presence of a mirror plane in $\{[N_3N_F]W(CO)_2\}Na(THF)_x$ and a pseudo-octahedral coordination environment around tungsten.

When the reduction of $[N_3N_F]W(OTf)$ was carried out under ^{13}CO, two peaks were observed in the ^{13}C NMR spectrum of the purple product at 246.2 ppm (J_{WC} = 112 Hz) and 242.4 ppm (J_{WC} = 215 Hz). IR spectra in THF of both labeled and unlabeled material showed two very broad CO stretches. The stretches are centered at 1952 and 1726 cm^{-1} in unlabeled material; they move to 1895 and 1682 cm^{-1} in ^{13}C-labeled material. If the reduction of $[N_3N_F]W(OTf)$ is carried out in ether instead of THF, and the crude reaction mixture is cooled to −40 °C under nitrogen, single crystals of $\{[N_3N_F]W(CO)_2\}Na(ether)_3$ may be obtained. Dissolving the crystals in any solvent which is not saturated with CO resulted in formation of $\{[N_3N_F]W(CO)\}Na(ether)_x$. An IR spectrum obtained in Nujol contained two sharp peaks at 1926 and 1716 cm^{-1}, which is consistent with the IR spectrum obtained in THF solution. All data are consistent with one CO being bound relatively strongly to tungsten and the other being labile.

A single crystal of $\{[N_3N_F]W(CO)_2\}Na(ether)_3$ was studied by X-ray diffraction. Crystallographic data and collection and refinement parameters are given in Table 4. A view of the structure along with the atom-labeling scheme is shown in Figure 3, while selected bond lengths, bond angles, and dihedral angles are listed in Table 5. The carbonyl ligand trans to N(4) has sodium bound to it. The C(1)−O(1) bond length (1.21 Å) and a W−C(1) bond length (1.89 Å) suggest that the anionic charge is localized on this CO. We believe that the relatively large J_{CW} (215 Hz) in the ^{13}C NMR spectrum of $\{[N_3N_F]W(CO)_2\}Na(THF)_x$ (vide supra) is found for the α-carbon atom in the more "reduced" CO ligand that has sodium bound to it. The C(2)−O(2) bond length of 1.16 Å and a W−C(2) distance of 2.06 Å are more consistent with a "normal" CO. On the basis of the bond length in gaseous CO (1.128 Å)[22] and typical values for C−O single and double bonds (1.42 and 1.22 Å, respectively),[23] the C(1)−O(1) bond order is close to 2, while the C(2)−O(2) bond order is between 2 and 3.

(22) Greenwood, N. N.; Earnshaw, A. *Chemistry of the Elements*; University Press: Cambridge, England, 1984.
(23) Carey, F. A.; Sundberg, R. J. *Advanced Organic Chemistry A*; Plenum Press: New York, 1990.

Table 4. Crystallographic Data, Collection Parameters, and Refinement Parameters for {[N_3N_F]W(CO)$_2$}[Na(ether)$_3$] and {[N_3N_F]W(CN-t-Bu)$_3$}BPh_4[a]

	{[N_3N_F]W(CO)$_2$}-[Na(ether)$_3$]	{[N_3N_F]W(CN-t-Bu)$_3$}BPh_4
empirical formula	$C_{38}H_{42}F_{15}N_4NaO_5W$	$C_{75}H_{83}BF_{15}N_7O_3W$
fw	1126.60	1610.14
cryst dimens (mm)	0.1 × 0.1 × 0.24	0.6 × 0.6 × 0.6
cryst syst	triclinic	monoclinic
a (Å)	11.4786(12)	11.6756(2)
b (Å)	11.7106(12)	24.3939(2)
c (Å)	19.202(2)	25.9702(5)
α (deg)	80.697(2)	90
β (deg)	74.554(2)	91.792(1)
γ (deg)	63.0820(10)	90
V (Å^3)	2215.8(4)	7393.0(2)
space group	*P*$\bar{1}$	*P*2$_1$/*c*
Z	2	4
D_{calcd} (Mg/m^3)	1.689	1.447
abs coeff (mm^{-1})	2.725	1.652
F_{000}	1116	3280
temp (K)	177(2)	183(2)
θ range (deg)	1.10−23.27	2.07−23.24
no. of rflns collected	9266	29 930
no. of indep rflns	6264 (*R*(int) = 0.0386)	10 559 (*R*(int) = 0.0279)
R1 ($I > 2\sigma(I)$)[b]	0.0449	0.0327
wR2 ($I > 2\sigma(I)$)[c]	0.1023	0.0659
R1 (all data)	0.0597	0.0355
wR2 (all data)	0.1122	0.0669
GOF	1.129	1.221

[a] All structures were solved on a Siemens SMART/CCD diffractometer using 0.717 03 Å Mo Kα radiation. [b] $R1 = \sum||F_o| - |F_c||/\sum|F_o|$. [c] $wR2 = [(\sum w(|F_o| - |F_c|)^2/\sum wF_o^2)]^{1/2}$.

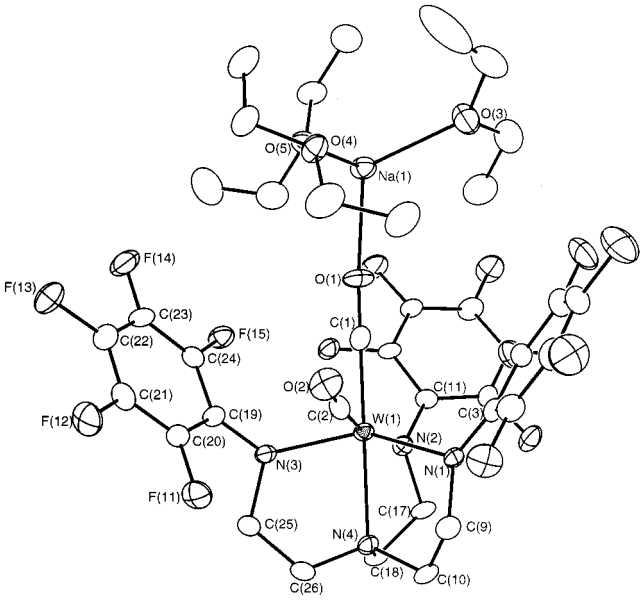

Figure 3. ORTEP drawing of {[N_3N_F]W(CO)$_2$}Na(ether)$_3$.

The coordination environment around tungsten is pseudo-octahedral, with the N(2)−W−N(3) and N(1)−W−N(2) angles reduced to 96 and 109°, respectively, compared to analogous angles close to 120° in trigonally symmetric complexes such as [N_3N_F]W(CN-t-Bu) (vide infra). The C(2)−W−N(1) angle is 76°, and the C(2)−W−N(3) angle is 81°. The neutral CO ligand (C(2)−O(2)) is pointed slightly up from the N(1)/N(2)/N(3) plane, with the C(1)−W−C(2) bond angle being 76° and the N(4)−W−C(2) angle being 109°. Also of interest is the fact that the W−N_{eq} bond lengths are all over 2 Å, varying in length from 2.04 to 2.14 Å. In structurally characterized group 6 complexes with C_3 symmetry, M−N_{eq} bond lengths are all ∼1.97 Å (± 0.02 Å). The long and unequal W−N_{eq} bond lengths in {[N_3N_F]W(CO)$_2$}Na(ether)$_3$ can be ascribed in part to steric crowding at the six-coordinate metal center.

Table 5. Selected Bond Lengths, Angles, and Dihedral Angles for {[N_3N_F]W(CO)$_2$}Na(ether)$_3$

Bond Lengths (Å)

W−C(1)	1.889(9)	W−N(4)	2.286(6)
W−C(2)	2.057(10)	C(1)−O(1)	1.207(9)
W−N(1)	2.136(6)	O(1)−Na	2.224(6)
W−N(2)	2.077(6)	C(2)−O(2)	1.159(10)
W−N(3)	2.040(6)		

Bond Angles (deg)

C(1)−W−C(2)	76.0(3)	N(1)−W−N(4)	77.5(2)
C(1)−W−N(1)	105.1(3)	N(2)−W−N(3)	109.2(3)
C(1)−W−N(2)	99.2(3)	N(2)−W−N(4)	76.4(2)
C(1)−W−N(3)	100.5(3)	N(3)−W−N(4)	79.3(2)
C(1)−W−N(4)	175.3(3)	W−N(1)−C(3)	123.3(5)
C(2)−W−N(1)	76.0(3)	W−N(2)−C(11)	125.9(5)
C(2)−W−N(2)	168.8(3)	W−N(3)−C(19)	124.7(5)
C(2)−W−N(3)	81.8(3)	C(1)−O(1)−Na	172.3(6)
C(2)−W−N(4)	108.6(3)	W−C(1)−O(1)	179.1(7)
N(1)−W−N(2)	95.9(2)	W−C(2)−O(2)	171.8(7)
N(1)−W−N(3)	140.5(2)		

Dihedral Angles (deg)

N(4)−W−N(1)−C(3)	173.8(6)	N(4)−W−N(3)−C(19)	151.4(6)
N(4)−W−N(2)−C(11)	172.2(6)		

When a THF solution of [N_3N_F]W(CO) is stirred over 1 equiv of sodium amalgam for 1 h, and Me_3SiCl is then added, brown, crystalline, diamagnetic [N_3N_F]W≡COSiMe_3 can be isolated in good yield (Scheme 2). The ^{13}C NMR spectrum of [N_3N_F]W≡COSiMe_3 shows a resonance characteristic of an alkylidyne carbon atom at 216.9 ppm. For comparison the alkylidyne carbon atom resonance is found at 214.1 ppm in [N_3N]W≡COSiMe_3.[14]

[N_3N_F]W(CO) reacts with V(Mes)$_3$(THF)[24] in toluene at room temperature to yield [N_3N_F]W(CO)V(Mes)$_3$ in high yield as a black crystalline solid. The effective magnetic moment of [N_3N_F]W(CO)V(Mes)$_3$ at 22 °C was found to be 2.1 ± 0.1 μ_B by the Evans method. Broadened and slightly shifted ^{1}H NMR resonances for the mesityl rings are observed at 17.5, 16.2, and 6.6 ppm, while resonances for the [N_3N_F]W half of the molecule are located at the normal diamagnetic positions. Therefore, the paramagnetism can be ascribed to the vanadium center in [N_3N_F]W(CO)V(Mes)$_3$. No ^{13}C resonance for the CO ligand could be observed in [N_3N_F]W(^{13}CO)V(Mes)$_3$, and no band that can be assigned to the C−O stretch could be identified in the IR spectrum.

Crystals of [N_3N_F]W(CO)V(Mes)$_3$ suitable for X-ray diffraction were obtained from toluene at −40 °C. Views of the structure are shown in Figure 4. Crystallographic data can be found in Table 2 and selected interatomic distances and angles in Table 6. The structure is not of high quality (only W, V, O, N, and F atoms were refined anisotropically); therefore, errors are too large to discuss bond lengths and angles in detail. A description of this complex as a "vanadoxyalkylidyne" complex, [N_3N_F]W≡COV(Mes)$_3$, would appear to be justified on the basis of the W−C(1) bond length of 1.88(2) Å and chemical shifts

(24) Seidel, W.; Kreisel, G. *Z. Anorg. Allg. Chem.* **1977**, *435*, 146.

Table 6. Selected Interatomic Distances (Å) and Angles (deg) for $[N_3N_F]W(CO)V(Mes)_3$ and $[N_3N_F]W(CN\text{-}t\text{-}Bu)$

$[N_3N_F]W(CO)V(Mes)_3$		$[N_3N_F]W(CN\text{-}t\text{-}Bu)$	
W−C(1)	1.88(2)	W−C(7)	1.913(11)
W−N(1)	1.98(2)	W−N(1)	1.975(8)
W−N(2)	1.98(2)	W−N(2)	1.967(8)
W−N(3)	1.95(2)	W−N(3)	1.980(8)
W−N(4)	2.31(2)	W−N(4)	2.243(8)
O−C(1)	1.19(2)	C(7)−N(5)	1.249(14)
V−O	1.824(14)	N(5)−C(8)	1.420(15)
W−N(1)−C(11)	126.6(13)	W−N(1)−C(11)	127.9(6)
W−N(2)−C(21)	124.9(13)	W−N(2)−C(21)	124.4(7)
W−N(3)−C(31)	127.4(13)	W−N(3)−C(31)	125.5(6)
N(3)−W−N(1)	116.4(7)	N(3)−W−N(1)	117.5(3)
N(2)−W−N(3)	118.4(7)	N(2)−W−N(3)	117.8(3)
N(2)−W−N(1)	114.9(7)	N(2)−W−N(1)	114.7(3)
N(4)−W−N(3)	80.1(8)	N(4)−W−N(3)	79.7(3)
N(3)−W−C(1)	101.0(8)	N(3)−W−C(7)	100.8(4)
N(2)−W−C(1)	99.8(8)	N(2)−W−C(7)	99.4(3)
W−C(1)−O	178(2)	W−C(7)−N(5)	172.1(8)
C(1)−O−V	176(2)	C(7)−N(5)−C(8)	132.2(10)
N(4)−W−N(2)−C(21)	176[a]	N(4)−W−N(2)−C(21)	169[a]
N(4)−W−N(1)−C(11)	179[a]	N(4)−W−N(1)−C(11)	179[a]
N(4)−W−N(3)−C(31)	178[a]	N(4)−W−N(3)−C(31)	173[a]
V−C(41)	2.05(2)		
V−C(51)	2.03(2)		
V−C(61)	2.05(2)		
C(14)−C(43)	3.55[a]		
C(34)−C(55)	3.32[a]		
C(24)−C(63)	3.41[a]		
C(33)−C(55)	3.64[a]		

[a] Obtained from a Chem 3D model.

for the ligand protons in the proton NMR spectrum and C_6F_5 fluorines in the ^{19}F NMR spectra that are characteristic of diamagnetic compounds, as noted above. The metrical parameters for the triamidoamine side of the molecule are all typical of triamidoamine molecules in which there is little steric strain; i.e., the N(4)−W−N_{eq}−C_6F_5 dihedral angles are all close to 180°. The mesityl rings on vanadium adopt a propeller-like orientation, possibly in order to minimize steric interactions between the ortho methyl groups present on the rings. The V−O distance of 1.824(14) Å is similar to that observed for some vanadium alkoxides,[25] and the geometry at the vanadium center is nearly tetrahedral. As a point of reference the V═O bond length in $(Mes)_3V{=}O$ was found to be 1.575(4) Å.[26] Both the W−C(1)−O and V−O−C(1) angles are close to 180°. The mesityl rings are roughly eclipsed with the C_6F_5 rings, although they do not lie perfectly parallel to one other (Figure 4b). Distances between the mesityl ring carbons and the C_6F_5 ring carbons that range from 3.3 to 3.5 Å suggest that there is some degree of interaction between the mesityl and pentafluorophenyl rings.[27−29]

Synthesis and Reactivity of Neutral $[N_3N_F]M$ (M = Mo, W) and Cationic Isocyanide Complexes. Complexes that contain one t-BuNC or ArNC (Ar = 2,6-dimethylphenyl) can be prepared by reducing $[N_3N_F]M$-(OTf) complexes (M = Mo, W) in the presence of the

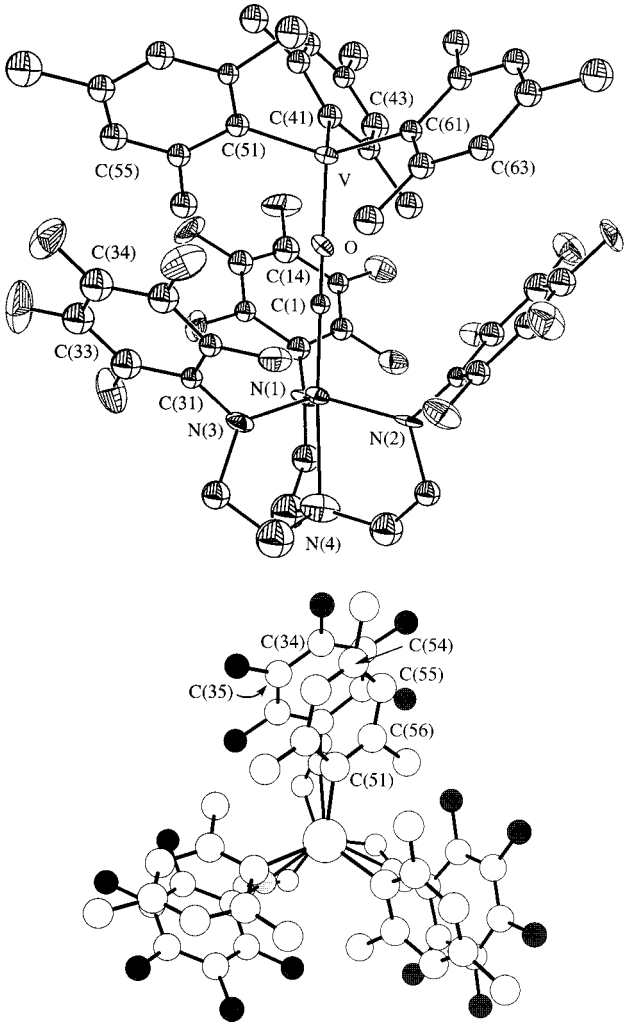

Figure 4. (a, top) ORTEP drawing of $[N_3N_F]W(CO)V(Mes)_3$. (b, bottom) Top view (Chem 3D) of $[N_3N_F]W(CO)V(Mes)_3$.

isocyanide (Scheme 3; Table 1). All complexes are orange paramagnetic crystalline solids. We have also shown that $[N_3N_F]W(CN\text{-}t\text{-}Bu)$ can be formed by employing $[N_3N_F]WCl$ and 1 equiv of sodium amalgam in the presence of *tert*-butyl isocyanide. The meta fluorine resonances are found near −160 ppm in the ^{19}F NMR spectra, which is about 35 ppm upfield of where they are found in neutral d^2 complexes such as $[N_3N_F]WCl$. Infrared absorptions that can be attributed to an isocyanide stretch are observed at unusually low energies for a coordinated isocyanide ligand,[30] consistent with extensive π back-bonding into the isocyanide ligand. The isocyanide stretch is found at lower energies for the W compounds, as expected. $[N_3N_F]W(CN\text{-}t\text{-}Bu)$ is also always contaminated with a *trace* (<5% by NMR) of a diamagnetic impurity, although the presence of this impurity did not prevent successful C, H, and N analysis. The nature of this impurity is not known. A SQUID measurement on $[N_3N_F]W(CN\text{-}t\text{-}Bu)$ revealed that it is a one-electron Curie magnet down to 5 K (μ = 1.74 μ_B), as found for $[N_3N]Mo(CN\text{-}t\text{-}Bu)$. Solution magnetic susceptibility measurements using the Evans method yielded magnetic moments ranging from 2.2 to

(25) Carrano, C. J.; Mohan, M.; Holmes, S. M.; de la Rosa, R.; Butler, A.; Charnock, J. M.; Garner, C. D. *Inorg. Chem.* **1994**, *33*, 646.
(26) Vivanco, M.; Ruiz, J.; Floriani, C.; Chiesi-Villa, A.; Rizzoli, C. *Organometallics* **1993**, *12*, 1802.
(27) Williams, J. H. *Acc. Chem. Res.* **1993**, *26*, 593.
(28) Dahl, T. *Acta Chem. Scand.* **1994**, *48*, 95.
(29) Coates, G. W.; Dunn, A. R.; Henling, L. M.; Dougherty, D. A.; Grubbs, R. H. *Angew. Chem., Int. Ed. Engl.* **1997**, *36*, 248.
(30) Malatesta, L.; Bonati, F. *Isocyanide Complexes of Metals*; Wiley: New York, 1969; Vol. IV.

Scheme 3

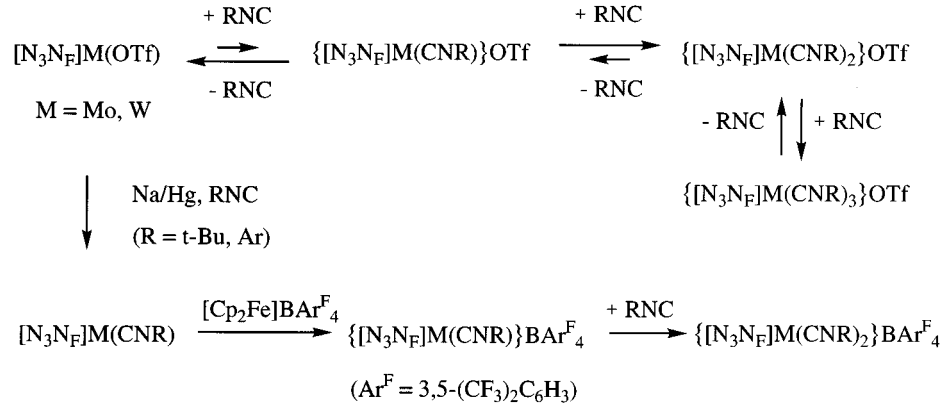

2.4 μ_B for the four isocyanide complexes, all of which are in the proper range for one unpaired electron.

A single-crystal X-ray study of $[N_3N_F]$W(CN-*t*-Bu) revealed it to have the structure shown in Figure 5. Crystallographic data can be found in Table 2 and selected interatomic distances and angles in Table 6. The metrical parameters for the triamidoamine side of the molecule are all typical for complexes of this type and consistent with little steric strain in the complex that results from crowding within the trigonal pocket. For example, the N(4)−W−N_{eq}−C angles are 169, 179, and 173°, and the N_{eq}−W−N_{eq}' angles are 117, 118, and 115°. The *tert*-butyl group is tipped away from the C_6F_5 ring attached to N(2) and between the other two C_6F_5 rings. The W−C(7) distance (1.913(11) Å), the C(7)−N(5) distance (1.249(14) Å), and the C(7)−N(5)−C(8) angle (132.2(10)°) are all more consistent with a W(V) "azavinylidene" description, i.e., $[N_3N_F]$W=C=N-*t*-Bu, than with an isocyanide complex of W(III). The azavinylidene description is also consistent with the presence of one unpaired electron, as noted above. The relative stability of $[N_3N_F]$W(CN-t-Bu) toward loss of a *tert*-butyl radical should be compared with the formation of $[N_3N]$Mo(CN) upon heating $[N_3N]$Mo(CN-t-Bu).

Reduction of $[N_3N_F]$MoCl by sodium amalgam in the presence of *n*-butyl isocyanide yields red, crystalline $[N_3N_F]$Mo(CN-*n*-Bu) in good yield (Table 1). A trace of diamagnetic material is present in spectra of $[N_3N_F]$Mo(CN-*n*-Bu), although its presence did not prevent successful C, H, and N analyses. The CN absorptions in all three $[N_3N_F]$Mo(CNR) (R = t-Bu, Ar, *n*-Bu) complexes are found between 1777 and 1790 cm^{-1} in Nujol. Comparison with the CN stretching frequency in $[N_3N]$Mo(CNAr) (1740 cm^{-1} in Nujol) suggests that the $[N_3N_F]^{3-}$ ligand overall leads to less back-bonding to a π acceptor ligand than $[N_3N]^{3-}$ ligand, as one might expect.

When $[N_3N_F]$WCl is treated with sodium amalgam in the presence of *n*-butyl isocyanide under conditions identical with those used to synthesize $[N_3N_F]$Mo(CN-*n*-Bu), a paramagnetic species can be observed by ^{19}F NMR after ~1 h, whose ^{19}F chemical shifts and peak widths are similar to those observed for $[N_3N_F]$Mo(CN-*n*-Bu). Therefore, we propose that $[N_3N_F]$W(CN-*n*-Bu) is present at this point. However, attempts to isolate and purify this product by recrystallization from dichloromethane led to increasing contamination with one or more diamagnetic impurities. So far we have not been able to isolate $[N_3N_F]$W(CN-*n*-Bu) in pure form.

Oxidation of $[N_3N_F]$M(CNR) compounds with $[Cp_2Fe]BAr^F_4$ (Ar^F = 3,5-$(CF_3)_2C_6H_3$) in CH_2Cl_2 produced paramagnetic monocations in high yields (Scheme 3; Table 1). Resonances in the ^{1}H and ^{19}F NMR spectra of these compounds are considerably broader than those for $[N_3N_F]$M(CNR) compounds, and no resonance for ortho fluorines is visible in ^{19}F NMR spectra. NMR resonances are much sharper in the spectra of tungsten complexes than in the spectra of molybdenum complexes, as is routinely the case.[2,5,8] The isocyanide absorptions in the IR spectra of all four cations are found near the absorption for free isocyanide, indicating little back-bonding from the cationic metal centers. Solution magnetic susceptibility measurements (Evans method) yielded magnetic moments ranging from 2.8 to 3.3 μ_B for the four cations, all of which are in the proper range for two unpaired electrons. Magnetic data are consistent with a description as d^2 M(IV) complexes rather than d^0 M(VI) azavinylidene complexes. Similar compounds are obtained if the oxidation is performed with $[Cp_2Fe]BPh_4$, although the solubility of these complexes in common organic solvents is too low to permit full characterization.

Oxidation of $[N_3N_F]$W(CN-t-Bu) with ferrocenium triflate affords a THF-soluble, diamagnetic species in 50% yield that we formulate as $\{[N_3N_F]W(CN\text{-}t\text{-}Bu)_2\}$OTf on the basis of spectroscopic and analytical data. The remaining 50% of the tungsten is found in the form of relatively insoluble $[N_3N_F]$W(OTf). Proton, carbon, and fluorine NMR spectra suggest that $\{[N_3N_F]W(CN\text{-}t\text{-}Bu)_2\}$OTf has C_3 symmetry (equivalent isocyanide groups). The isocyanide carbon resonance in the ^{13}C NMR spectrum is found at 157.3 ppm, which is 3 ppm downfield of free isocyanide.[31] We speculate that this product is a six-coordinate cation in which the trigonal symmetry of the ligand core is maintained and that the two isocyanides equilibrate on the NMR time scale without dissociating from the metal. Two stretches are found in the IR spectrum at 2111 and 2104 cm^{-1}. Oxidation of $[N_3N_F]$W(CNAr) with ferrocenium triflate affords a 1:1 mixture of $\{[N_3N_F]W(CNAr)_2\}$OTf and $[N_3N_F]$W(OTf) in a completely analogous fashion. The isocyanide carbon resonance in the ^{13}C NMR spectrum of $\{[N_3N_F]W(CNAr)_2\}$OTf is found at 174.7 ppm, 4 ppm downfield of free isocyanide.[31] The diamagnetic nature of $\{[N_3N_F]W(CNR)_2\}$OTf species can be attributed to

(31) Caro, C. F.; Hitchcock, P. B.; Lappert, M. F.; Layh, M. *Chem. Commun.* **1998**, 1297.

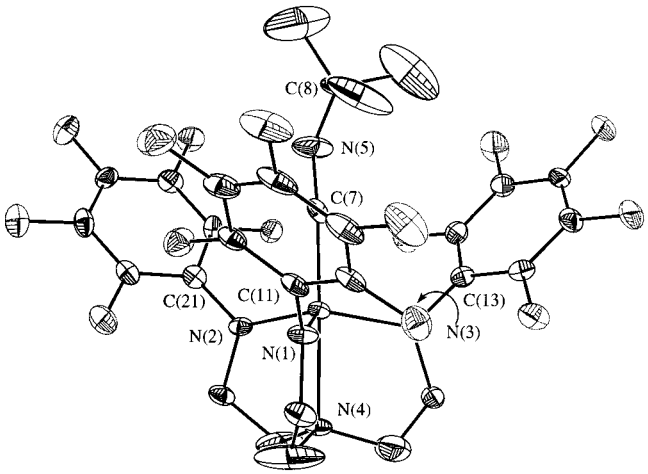

Figure 5. ORTEP drawing of $[N_3N_F]W(CN\text{-}t\text{-}Bu)$.

formation of a pseudooctahedral species in which the d_{xz} and d_{yz} orbitals are no longer degenerate. NMR spectra in $CDCl_3$ down to −60 °C show that the isocyanide ligands remain apparently equivalent, although the remainder of the spectrum is consistent with the known[2,5,8,32] "locking" of the backbone of the $[N_3N_F]^{3-}$ ligand in one C_1 conformation.

We believe that the initial product of the oxidation of $[N_3N_F]W(CN\text{-}t\text{-}Bu)$ with $[Cp_2Fe]OTf$ is $\{[N_3N_F]W(CN\text{-}t\text{-}Bu)\}OTf$, by analogy with $\{[N_3N_F]W(CN\text{-}t\text{-}Bu)\}BAr^F{}_4$. However, the metal center in $\{[N_3N_F]W(CN\text{-}t\text{-}Bu)\}OTf$ must be attacked by triflate and the isocyanide lost to yield $[N_3N_F]W(OTf)$. The free isocyanide then captures the remaining $\{[N_3N_F]W(CN\text{-}t\text{-}Bu)\}OTf$, producing the 50% yield of $\{[N_3N_F]W(CN\text{-}t\text{-}Bu)_2\}OTf$, from which the isocyanide is not lost readily (Scheme 3). This proposal is supported by the finding that $\{[N_3N_F]W(CNR)_2\}^+$ complexes can be prepared straightforwardly by treating $[N_3N_F]W(OTf)$ with 2 equiv of isocyanide in THF. Yields in excess of 80% are obtained within a few minutes.

Diamagnetic $\{[N_3N_F]W(CNR)_2\}BAr^F{}_4$ complexes can be prepared by addition of 1 equiv of the appropriate isocyanide to $\{[N_3N_F]W(CNR)\}BAr^F{}_4$ (Scheme 3). The ^1H and ^{19}F NMR spectra, and the position of the CN stretches in the IR spectrum of $\{[N_3N_F]W(CNAr)_2\}BAr^F{}_4$, for example, are similar to those of $\{[N_3N_F]W(CNAr)_2\}OTf$.

Oxidation of $[N_3N_F]Mo(CN\text{-}t\text{-}Bu)$ or $[N_3N_F]Mo(CNAr)$ with ferrocenium triflate yielded only $[N_3N_F]Mo(OTf)$, in 81% and 88% yield, respectively. $\{[N_3N_F]Mo(CNR)_2\}OTf$ complexes can be prepared by adding isocyanide to $[N_3N_F]Mo(OTf)$, but at least 3 equiv of isocyanide is required before all of the insoluble $[N_3N_F]Mo(OTf)$ disappears. After THF is removed and the residue is redissolved in dichloromethane, insoluble $[N_3N_F]Mo(OTf)$ forms again but disappears upon addition of more isocyanide. Isolated yields of the $\{[N_3N_F]Mo(CNR)_2\}OTf$ complexes are only about 60%. These data are consistent with a high lability of the second equivalent of isocyanide in $\{[N_3N_F]Mo(CNR)_2\}OTf$ and decomposition of $\{[N_3N_F]Mo(CNR)\}OTf$ to yield free isocyanide and insoluble $[N_3N_F]Mo(OTf)$ (Scheme 3). In contrast, as noted above, $\{[N_3N_F]W(CNR)_2\}OTf$ complexes are stable to reactions involving loss of isocyanide, at least under mild conditions (22 °C), and $\{[N_3N_F]Mo(CNR)_2\}BAr^F{}_4$ complexes are stable as a consequence of the poor coordinating ability and large size of the $BAr^F{}_4{}^-$ ion.

The NMR spectra of $\{[N_3N_F]Mo(CNR)_2\}OTf$ are complicated by behavior involving formation of $\{[N_3N_F]Mo(CNR)\}OTf$ and $\{[N_3N_F]Mo(OTf)$, as mentioned above, especially at temperatures below 0 °C where $[N_3N_F]Mo(OTf)$ crystallizes out, as is readily ascertained by visual inspection. At temperatures above 20 °C, a resonance for only one type of isocyanide is observed. If free isocyanide is added to the sample, the single resonance shifts downfield, closer to that of free isocyanide, suggesting rapid exchange of free and coordinated isocyanide. It should be noted that the resonances in the spectra are broadened by the paramagnetism of $\{[N_3N_F]Mo(CNR)\}OTf$ and (to a lesser extent if it has crystallized out of the sample) $[N_3N_F]Mo(OTf)$. There are small differences between ArNC and t-BuNC complexes that can be traced to differences in basicity and steric bulk. For example, in ^1H NMR spectra of $\{[N_3N_F]Mo(CNAr)_2\}OTf$, resonances for free and bound ArNC are observed below 0 °C. The reason, we propose, is that the equilibrium between $\{[N_3N_F]Mo(CNAr)_2\}OTf$ and $[N_3N_F]Mo(OTf)$ plus free ArNC is shifted further to the right for the more poorly coordinating ArNC and the rate of ArNC exchange is slow on the NMR time scale. In contrast, only one broad *tert*-butyl resonance can be observed in the ^1H NMR spectrum of $\{[N_3N_F]Mo(CN\text{-}t\text{-}Bu)_2\}OTf$ down to −60 °C. Although a ^{13}C NMR spectrum can be obtained for $\{[N_3N_F]Mo(CN\text{-}t\text{-}Bu)_2\}OTf$ at 0 °C, no isocyanide carbon resonance can be observed. Both $\{[N_3N_F]Mo(CNR)_2\}OTf$ compounds can be recrystallized from dichloromethane in the presence of excess isocyanide to give analytically pure material. Solid-state IR spectra (Nujol) of the recrystallized material indicates the presence of two isocyanide resonances, analogous to those observed in the corresponding (stable) W complexes. Resonances in NMR spectra of $\{[N_3N_F]Mo(CNR)_2\}BAr^F{}_4$ complexes are broad, as a consequence of formation of a small amount of paramagnetic $\{[N_3N_F]Mo(CNR)\}BAr^F{}_4$.

The low-temperature spectrum of $\{[N_3N_F]Mo(CN\text{-}t\text{-}Bu)_2\}OTf$ in the presence of added t-BuNC shows new features that suggest that yet another compound is being formed reversibly. On the basis of NMR resonances analogous to those found for $\{[N_3N_F]W(CN\text{-}t\text{-}Bu)_3\}OTf$ (vide infra), we propose that $\{[N_3N_F]Mo(CN\text{-}t\text{-}Bu)_3\}OTf$ is being formed at low temperatures. Predictably, it is more unstable toward loss of isocyanide than is $\{[N_3N_F]W(CN\text{-}t\text{-}Bu)_3\}OTf$. $\{[N_3N_F]Mo(CNAr)_3\}OTf$ apparently does not form as readily as $\{[N_3N_F]Mo(CN\text{-}t\text{-}Bu)_3\}OTf$ as a consequence of the poorer basicity of ArNC relative to t-BuNC.

Treatment of $[N_3N_F]W(OTf)$ with 3 equiv or more of *tert*-butyl isocyanide yields diamagnetic, emerald green $\{[N_3N_F]W(CN\text{-}t\text{-}Bu)_3\}OTf$, a composition we propose on the basis of its similarity to a structurally characterized tetraphenylborate derivative described below. The ^1H, ^{13}C, and ^{19}F NMR spectra of $\{[N_3N_F]W(CN\text{-}t\text{-}Bu)_3\}OTf$ are all indicative of it not being C_3 symmetric. Two resonances corresponding to *tert*-butyl groups are found in the ^1H NMR spectrum in a 2:1 ratio. The lower intensity downfield peak is broad at room temperature,

(32) Reid, S. M.; Neuner, B.; Schrock, R. R.; Davis, W. M. *Organometallics* **1998**, *17*, 4077.

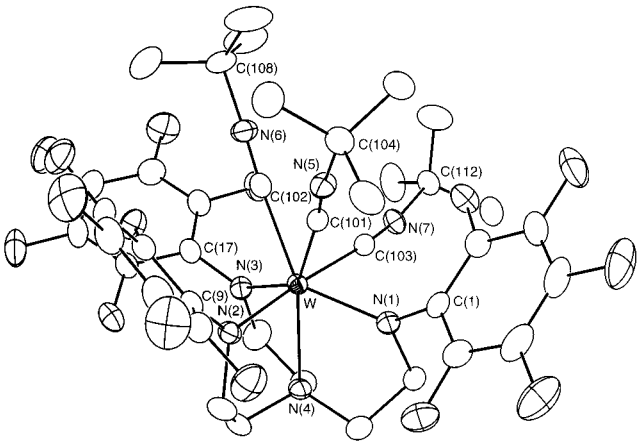

Figure 6. ORTEP view of the cation in $\{[N_3N_F]W(CN\text{-}t\text{-}Bu)_3\}BPh_4$ (35% probability level).

and the region of the methylene backbone protons consists of several broad, featureless lumps. Lowering the temperature to −20 °C results in the sharpening of the resonances in the methylene backbone region to yield five resonances in a 2:2:2:4:2 ratio; little fine structure can be resolved. Temperature-dependent ^{1}H NMR spectra suggest that the isocyanide ligand that gives rise to the downfield resonance is the one that is labile at room temperature on the NMR time scale. Six different resonances for the ligand backbone carbons are observed in the ^{13}C NMR spectrum, and the ^{19}F NMR spectrum in THF features a 2:1 ratio of peaks, similar to that observed in $\{[N_3N_F]W(CO)_2\}Na(THF)_x$. Addition of $[N_3N_F]W(OTf)$ to $\{[N_3N_F]W(CN\text{-}t\text{-}Bu)_3\}OTf$ resulted in formation of $\{[N_3N_F]W(CN\text{-}t\text{-}Bu)_2\}OTf$; conversely, addition of 1 equiv of t-BuNC to $\{[N_3N_F]W(CN\text{-}t\text{-}Bu)_2\}$-OTf yields $\{[N_3N_F]W(CN\text{-}t\text{-}Bu)_3\}OTf$ quantitatively.

The $\{[N_3N_F]W(CN\text{-}t\text{-}Bu)_3\}BPh_4$ complex could be prepared by oxidation of $[N_3N_F]W(CN\text{-}t\text{-}Bu)$ with $[Cp_2Fe]$-BPh_4 followed by addition of excess isocyanide to the resulting cation. Single crystals were obtained from THF. Crystallographic data and collection and refinement parameters are given in Table 4. A view of the structure of the cation, along with the atom-labeling scheme, is shown in Figure 6, while selected bond lengths, bond angles and dihedral angles are listed in Table 7. The highly distorted geometry is roughly a pentagonal bipyramid with C(103) and N(2) occupying the axial sites. The overall structure is similar to that of $\{[N_3N_F]W(CO)_2\}Na(ether)_3$, except two ligands are found in the apical pocket instead of one. The CN bond lengths in all three isocyanide ligands are statistically equivalent. However, the W−C(103) bond length is slightly longer than the other two, suggesting that the equatorial isocyanide is more weakly bound. The two ligand arms cis to the equatorial isocyanide are twisted to a significant degree, judging from the N(4)−W−N(1)−C(1) and N(4)−W−N(3)−C(17) dihedral angles of 161 and 154°, respectively. The W−N(amide) bond lengths are relatively long, as found in $\{[N_3N_F]W(CO)_2\}Na$-$(ether)_3$. This extremely crowded complex can form as a consequence of the relatively high W−isocyanide bond strength and superior donor ability of the t-BuNC ligand. As noted above, resonances consistent with the formation of $\{[N_3N_F]Mo(CN\text{-}t\text{-}Bu)_3\}OTf$ can only be observed in low-temperature NMR spectra; i.e., $\{[N_3N_F]$-$Mo(CN\text{-}t\text{-}Bu)_3\}^+$ loses t-BuNC much more readily than does $\{[N_3N_F]W(CN\text{-}t\text{-}Bu)_3\}^+$.

Table 7. Selected Bond Lengths, Bond Angles, and Dihedral Angles for $\{[N_3N_F]W(CN\text{-}t\text{-}Bu)_3\}BPh_4$

Bond Lengths (Å)			
W−C(101)	2.118(4)	W−N(3)	2.068(3)
W−C(102)	2.128(4)	W−N(4)	2.253(3)
W−C(103)	2.182(4)	C(101)−N(5)	1.158(5)
W−N(1)	2.070(3)	C(102)−N(6)	1.150(5)
W−N(2)	2.043(3)	C(103)−N(7)	1.146(5)

Bond Angles (deg)			
C(101)−W−C(102)	65.73(14)	N(1)−W−N(2)	99.66(12)
C(101)−W−C(103)	101.57(14)	N(1)−W−N(3)	140.41(12)
C(101)−W−N(1)	76.70(13)	N(1)−W−N(4)	75.66(11)
C(101)−W−N(2)	83.47(13)	N(2)−W−N(3)	96.98(12)
C(101)−W−N(3)	141.09(13)	N(2)−W−N(4)	77.76(12)
C(101)−W−N(4)	143.20(13)	N(3)−W−N(4)	73.17(12)
C(102)−W−C(103)	79.80(14)	W−C(101)−N(5)	172.8(3)
C(102)−W−N(1)	131.98(13)	W−C(102)−N(6)	176.3(3)
C(102)−W−N(2)	104.41(13)	W−C(103)−N(7)	174.8(3)
C(102)−W−N(3)	76.67(13)	W−N(1)−C(1)	135.6(2)
C(102)−W−N(4)	149.78(13)	W−N(2)−C(9)	127.2(2)
C(103)−W−N(1)	79.63(13)	W−N(3)−C(17)	132.2(2)
C(103)−W−N(2)	174.53(13)	C(101)−N(5)−C(104)	173.7(4)
C(103)−W−N(3)	80.47(13)	C(102)−N(6)−C(108)	175.5(4)
C(103)−W−N(4)	96.84(13)	C(103)−N(7)−C(112)	169.7(4)

Dihedral Angles (deg)			
N(4)−W−N(1)−C(1)	161.1(4)	N(4)−W−N(3)−C(17)	154.1(4)
N(4)−W−N(2)−C(9)	176.1(3)		

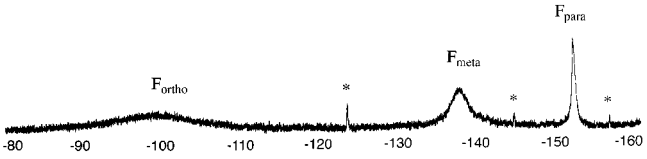

Figure 7. ^{19}F NMR spectrum of $[N_3N_F]W(C_2H_4)$ (asterisks denote paramagnetic impurity).

Synthesis of $[N_3N_F]^{3-}$ Ethylene Complexes. Reduction of $[N_3N_F]Mo(OTf)$ with sodium amalgam under excess ethylene yields a mixture of paramagnetic and diamagnetic compounds from which no compound could be identified or isolated. In contrast, $[N_3N_F]W(OTf)$ reacts slowly with sodium amalgam in THF under ∼3 atm of ethylene to give paramagnetic $[N_3N_F]W(C_2H_4)$ in good yield (Table 1). Although no ^{1}H NMR resonance could be observed readily, three ^{19}F resonances could be observed (Figure 7), the one which we assign to the ortho fluorines at −100 ppm being ∼2500 Hz wide at half-height. Even after reprecipitation of $[N_3N_F]W(C_2H_4)$ from solution, it contains a trace of an impurity (denoted by asterisks in Figure 7). Preparation of analogous $[N_3N_F]W$(olefin) complexes in which the olefin is 2-butene or cyclopentene was not successful. The magnetic moment of $[N_3N_F]W(C_2H_4)$ (measured in solution at 22 °C by the Evans method) is 1.8 μ_B, consistent with one unpaired electron.

Oxidation of $[N_3N_F]W(C_2H_4)$ with $[Cp_2Fe]OTf$ in THF led to the formation of diamagnetic $\{[N_3N_F]W(C_2H_4)\}$-OTf as a red powder in high yield. The ^{1}H NMR spectrum displays a peak at 3.10 ppm for the ethylene ligand and ^{1}H and ^{19}F resonances that are characteristic of diamagnetic $[N_3N_F]^{3-}$ complexes. $\{[N_3N_F]W(C_2H_4)\}$-OTf is diamagnetic as a consequence of ethylene breaking the pseudo C_3 symmetry through π back-bonding, leaving the other π type orbital (e.g., d_{xz}) empty. An alternative description, although one that is not re-

quired on the basis of the compound's diamagnetism, is a W(VI) metallacyclopropane complex.

Discussion

The electron-withdrawing power of the pentafluorophenyl ligand approximately counterbalances the greater reducing power of tungsten versus molybdenum, as evidenced by CO stretching frequencies that are approximately the same in $[N_3N_F]W(CO)$ (1846 cm^{-1} in Nujol) and in $[N_3N]Mo(CO)$ (1841 and 1832 cm^{-1} in Nujol; 1859 cm^{-1} in pentane). Therefore, since $[N_3N]Mo(N_2)$ is a known and stable molecule, we believed that $[N_3N_F]W(N_2)$ should be a stable species. The fact that we cannot prepare it by the reduction of $[N_3N_F]W(OTf)$ or $[N_3N_F]WCl$ under dinitrogen, while stronger trapping agents (L) lead to isolable $[N_3N_F]W(L)$ species, leads us to conclude that some irreversible side reaction competes with dinitrogen binding. Further evidence in support of this conclusion is that the unidentified paramagnetic product formed upon reduction of $[N_3N_F]W(OTf)$ under dinitrogen or argon is found in trace quantities, even in reactions that yield $[N_3N_F]W(L)$ species in relatively high yield, presumably as a consequence of competition between the side reaction and the reaction that yields $[N_3N_F]W(L)$ species. However, we also have not yet been able to prepare $[N_3N]W(N_2)$; therefore, the failure to form $[N_3N_F]W(N_2)$ ultimately may be traceable to a more profound difference between Mo and W complexes that contain triamidoamine ligands. It also should be noted that we have not observed $[N_3N_F]Mo(N_2)$ to date, since oxidation of $\{[N_3N_F]Mo(N_2)\}^-$ yields $\{[N_3N_F]Mo\}_2(\mu\text{-}N_2)$.[1] Therefore, we cannot predict whether reduced back-bonding to dinitrogen in hypothetical $[N_3N_F]Mo(N_2)$ relative to $[N_3N]Mo(N_2)$ in fact would limit its stability with respect to loss of dinitrogen.

One of the curious aspects of the work reported here is that some reductions to give M(III) species fail, even though the product can be formed via another route, while reductions to give M(III) species in the presence of other substrates are smooth. An example is the failure to reduce $[N_3N]MoCl$ with magnesium to give known $[N_3N]Mo(CO)$, while $[N_3N]Mo(C_2H_4)$ can be formed smoothly. Another example is that $[N_3N_F]W(CN\text{-}t\text{-}Bu)$ can be synthesized by reduction of $[N_3N_F]W(OTf)$ or $[N_3N_F]WCl$ in the presence of t-BuNC, while $[N_3N_F]W(CO)$ can only be prepared by reduction of $[N_3N_F]W(OTf)$. One logical mechanism of reduction is one-electron reduction of the M(IV) triamidoamine complex, followed by loss of an anion (chloride or triflate) to give a trigonal-monopyramidal M(III) complex and binding of the substrate (in either order). The other is initial displacement of chloride or triflate by the substrate followed by reduction of the resulting cation. For example, we know that $[N_3N_F]M(OTf)$ complexes react with isocyanides to yield cationic species, so reduction of $[N_3N_F]M(OTf)$ in the presence of isocyanides almost certainly proceeds via cationic species. However, in some situations more reducible cationic species might form to only a small extent, depending on the substrate in question and the leaving group on the metal, and might not be accessible if a poorer leaving group (chloride instead of triflate) or a substrate that is a poor nucleophile is employed. Nevertheless, the finding that $[N_3N]MoCl$ is reduced by magnesium under dinitrogen, while $[N_3N]MoCl$ is *not* reduced by magnesium under CO, is still puzzling to us. At this stage we can only speculate that the magnesium is poisoned by CO during the attempted reduction under the conditions employed.

Formation of M(II) anionic carbonyl complexes and siloxycarbyne complexes upon addition of chlorotrimethylsilane to them is not surprising in light of the propensity for tungsten and molybdenum triamidoamine complexes to form strong M≡E bonds (E = CR, N, P, As).[10] In general, however, siloxycarbyne complexes are rare.[33] Perhaps the best known examples have the formula $M(CO)(COSiR_3)(DMPE)_2$ (M = V,[34] Ta,[35,36] Nb[35]) and have been isolated as intermediates in the reductive coupling of CO to form alkoxy alkynes at V, Ta, and Nb centers.

Formation of $[N_3N_F]W{\equiv}COV(Mes)_3$ by addition of $V(Mes)_3$ to $[N_3N_F]W(CO)$ is related to the formation of siloxycarbyne complexes. Related reactions involving the $(Mes)_3V$ fragment are known. For example, $V(Mes)_3$ has been employed to bind dinitrogen in putative $(Mes)_3V(N_2)$ to yield $[(Mes)_3V(\mu\text{-}N_2)V(Mes)_3]$, which can be further reduced to yield complexes of the type $[(Mes)_3V(\mu\text{-}N_2)V(Mes)_3]^{n-}$ (n = 1, 2).[37] Two equivalents of $(Mes)_3V(THF)$ also have been employed to remove an oxygen atom from a chromium nitrosyl to give a chromium(VI) nitride and $(Mes)_3V(\mu\text{-}O)V(Mes)_3$.[38] However, we believe that the formation of $[N_3N_F]W{\equiv}COV(Mes)_3$ may be the only example of such a reaction in which vanadium remains in the product and in which vanadium has been oxidized by one electron, at least the only example of such a product that has been confirmed through an X-ray study.

Formation of a cyanide complex via dealkylation of an isocyanide complex has some precedent in the literature. For example, upon being refluxed in ethanol, $[(t\text{-}BuNC)_7Mo]^{2+}$ loses a carbonium ion to form $[(t\text{-}BuNC)_6Mo(CN)]^+$.[39] Reaction of $[(t\text{-}BuNC)_7Mo]^{2+}$ with zinc in THF yields $[(t\text{-}BuNC)_4Mo(t\text{-}BuHNCCNH\text{-}t\text{-}Bu)(CN)]^+$, a product in which both reductive coupling and dealkylation of the isocyanide ligands has occurred.[40] Perhaps the most closely related to the formation of $[N_3N]Mo(CN)$ is formation of *trans*-$Mo(CN)_2(Me_8[16]aneS_4)$ ($Me_8[16]aneS_4$ = 3,3,7,7,11,11,15,15,-octamethyl-1,5,9,13-tetrathiacyclohexadecane) from $Mo(CN)(t\text{-}BuNC)(Me_8[16]aneS_4)$ at −30 °C.[21]

A comparison of the IR stretching frequencies in $[N_3N]Mo(CN\text{-}t\text{-}Bu)$ (1838 cm^{-1}), $[N_3N]Mo(CNAr)$ (1740 cm^{-1}), $[N_3N_F]Mo(CN\text{-}t\text{-}Bu)$ (1787 cm^{-1}), and $[N_3N_F]Mo(CNAr)$ (1777 cm^{-1}) suggests that the first is somewhat high if all species are isostructural. Since $[N_3N_F]W(CN$-

(33) Dickson, R. S.; Ibers, J. A. *J. Am. Chem. Soc.* **1972**, *94*, 2988.
(34) Protasiewicz, J. D.; Lippard, S. J. *J. Am. Chem. Soc.* **1991**, *113*, 6564.
(35) Vrtis, R. N.; Liu, S.; Rao, C. P.; Bott, S. G.; Lippard, S. J. *Organometallics* **1991**, *10*, 275.
(36) Protasiewicz, J. D.; Bronk, B. S.; Masschelein, A.; Lippard, S. J. *Organometallics* **1994**, *13*, 1300.
(37) Ferguson, R.; Solari, E.; Floriani, C.; Osella, D.; Ravera, M.; Re, N.; Chiesi-Villa, A.; Rizzoli, C. *J. Am. Chem. Soc.* **1997**, *119*, 10104.
(38) Odom, A. L.; Cummins, C. C.; Protasiewicz, J. D. *J. Am. Chem. Soc.* **1995**, *117*, 6613.
(39) Giandomenico, C. M.; Hanau, L. H.; Lippard, S. J. *Organometallics* **1982**, *1*, 142.
(40) Dewan, J. C.; Giandomenico, C. M.; Lippard, S. J. *Inorg. Chem.* **1981**, *20*, 4069.

t-Bu) (1684 cm^{-1}) has been shown to contain a bent isocyanide ligand, we suspect that $[N_3N_F]W(CNAr)$ (1679 cm^{-1}) is structurally analogous. Unfortunately, none of the $[N_3N]Mo(CNR)$ or $[N_3N_F]Mo(CNR)$ complexes has been structurally characterized, and therefore we cannot say with certainty whether all species have a bent isocyanide. $[N_3N]Mo(CN\text{-}t\text{-}Bu)$ would seem most likely to have a linear isocyanide on the basis of IR data and the fact that the *tert*-butyl isocyanide probably is most resistant to bending in the crowded coordination pocket in $[N_3N]Mo(CN\text{-}t\text{-}Bu)$. Interestingly, the production of cyanide by dealkylation in this circumstance would not require extensive rehybridization about nitrogen. Therefore, a linear isocyanide in $[N_3N]$-$Mo(CN\text{-}t\text{-}Bu)$ might help explain the instability of $[N_3N]$-$Mo(CN\text{-}t\text{-}Bu)$ compared to the other isocyanide complexes reported here.

One of the most interesting aspects of the present study is the large number of complexes with coordination number greater than 5 that can be prepared, especially when the metal is tungsten. There appear to be two classes of six-coordinate complexes that contain a triamidoamine ligand. In one class are complexes in which the C_3 symmetry of the TREN ligand is maintained, and two additional ligands occupy the apical pocket. Structurally characterized complexes of this type include $[N_3N]W(cyclo\text{-}CHCH_2CH_2CH_2)$, $[N_3N]W(C_5H_8)$-(H),[8] and $[N_3N]W(CO)(H)$.[14] The two ligands in the apical pocket rotate rapidly with respect to the $[N_3N]$ ligand framework on the NMR time scale; therefore, the NMR spectra of these complexes appear to be C_3-symmetric. We place the $\{[N_3N_F]M(CNR)_2\}OTf$ complexes in this category.

Six-coordinate complexes in the second category adopt a pseudo-octahedral coordination geometry around the metal center in which an added ligand joins the three amide ligands in the equatorial plane. Prior to the current study, the only structurally characterized complex of this type was $[N_3N_F]W(O)(3,5\text{-}Me_2C_6H_3)$;[2] $\{[N_3N_F]W(CO)_2\}Na(ether)_3$ has a similar structure. Compounds that have not been structurally characterized but that we believe adopt similar structures on the basis of NMR data include $[N_3N]Mo(NTMS)(Me)$,[4] $[N_3N]Mo(NMe)(Me)$,[4] and $[N(CH_2CH_2NSiMe_3)_2(CH_2$-$CH_2NCH_3)]Mo\{NN(CH_3)_2\}(CH_3)$.[6] In complexes of this type a mirror plane passes through the unique ligand in the equatorial plane and the amide trans to it, and the ligand trans to the amine donor contains triply bound or pseudo triply bound C, N, or O. However, NMR spectra of complexes in solution are sometimes consistent with the complexes being C_3-symmetric on the NMR time scale, as in $[N_3N_F]W(O)(3,5\text{-}Me_2C_6H_3)$. In complexes with this geometry the $M-N_{eq}$ π bond that is lost must be compensated by multiple bonding between the metal and the axial ligand.

The only seven-coordinate complex containing a triamidoamine ligand to be prepared up to this point was $[N_3N]WH_3$.[14] Hydride ligands are small enough to fit into the apical pocket of that trigonally symmetric complex. This is not possible in $\{[N_3N_F]W(CN\text{-}t\text{-}Bu)_3\}$-$BPh_4$; thus, one of the isocyanides takes up a position in the triamido plane. As in the case of $\{[N_3N_F]W(CO)_2\}$-$Na(ether)_3$, one of the two $W-N(amide)$ π-bonds must be sacrificed, and $\{[N_3N_F]W(CN\text{-}t\text{-}Bu)_3\}BPh_4$ therefore becomes an 18-electron complex. The loss of the π bond is reflected in the lengthening of the $W-N_{eq}$ bond distances in comparison with those of a typical C_3-symmetric TREN complex. A seven-coordinate complex can be prepared only when the metal is tungsten and the ligand is *tert*-butyl isocyanide. Presumably both the ability of W to form stronger bonds than Mo and the strong electron donor properties of *tert*-butyl isocyanide are necessary to overcome the steric and electronic barriers associated with expansion of the coordination sphere.

Other triamidoamine ethylene complexes of the type reported here are known, in particular $[N_3N]Ta$-(C_2H_4)[41,42] and $[N_3N_F]Re(C_2H_4)$.[32,43] We were somewhat surprised that $\{[N_3N_F]W(C_2H_4)\}OTf$ is isolable, since $\{[N_3N]Mo(C_2H_4)\}OTf$ apparently loses ethylene and coordinates triflate to yield $[N_3N]Mo(OTf)$. However, the result is consistent with a greater degree of backbonding from the more reducing tungsten(IV) center to the ethylene ligand in $\{[N_3N_F]W(C_2H_4)\}OTf$ than in hypothetical $\{[N_3N]Mo(C_2H_4)\}OTf$, despite the presence of the more electron-withdrawing $[N_3N_F]^{3-}$ ligand. It is not surprising that $[N_3N_F]Mo(C_2H_4)$ cannot be isolated, because it combines the less reducing Mo(III) center with the electron-poor $[N_3N_F]^{3-}$ ligand.

Overall we were pleased to find that both $[N_3N_F]Mo$ and $[N_3N_F]W$ chemistry resemble $[N_3N]Mo$ chemistry and that differences could be readily understood in terms of periodic differences between Mo and W. We were also surprised to find the extent to which higher coordination numbers can be achieved in $[N_3N_F]^{3-}$ complexes and are eager to determine whether $[N_3N_F]^{3-}$ or related complexes therefore might be useful as catalysts in some simple catalytic reactions. Unfortunately, however, we have not been able to answer the question as to why the dinitrogen chemistry of $[N_3N_F]$-Mo is accessible (although $[N_3N_F]Mo(N_2)$ has not been observed), while the dinitrogen chemistry of $[N_3N_F]W$ so far has not been observed. In fact, there is still no example of a triamidoamine complex of tungsten that contains dinitrogen. We hope to revisit this question in the future as we explore the chemistry of accessible triamidoamine complexes of both metals that contain aryl substituents on the amido nitrogens other than C_6F_5.[11]

Experimental Procedures

General Details. All experiments were conducted under nitrogen in a Vacuum Atmospheres drybox, using standard Schlenk techniques, or on a high-vacuum line ($<10^{-4}$ Torr). Glassware was dried in a 135 °C oven overnight. Pentane was washed with HNO_3/H_2SO_4 (5/95 v/v), sodium bicarbonate, and water, dried over $CaCl_2$, and then distilled from sodium benzophenone with tetraglyme under nitrogen. Ether and THF were purified by sparging with nitrogen and passing through alumina columns.[44] Reagent grade benzene was distilled from sodium benzophenone under nitrogen. Toluene was distilled from molten sodium. Methylene chloride was distilled from CaH_2. All solvents were stored in the drybox over activated 4

(41) Freundlich, J.; Schrock, R. R.; Cummins, C. C.; Davis, W. M. *J. Am. Chem. Soc.* **1994**, *116*, 6476.
(42) Freundlich, J. S.; Schrock, R. R.; Davis, W. M. *Organometallics* **1996**, *15*, 2777.
(43) Neuner, B.; Schrock, R. R. *Organometallics* **1996**, *15*, 5.
(44) Pangborn, A. B.; Giardello, M. A.; Grubbs, R. H.; Rosen, R. K.; Timmers, F. J. *Organometallics* **1996**, *15*, 1518.

Å molecular sieves. Deuterated solvents were freeze−pump−thaw-degassed and vacuum-transferred from an appropriate drying agent.

NMR data were obtained at 300 or 500 MHz (^{1}H), 125.8 MHz (^{13}C), and 282 MHz (^{19}F). ^{1}H and ^{13}C data are listed in parts per million downfield from tetramethylsilane and were referenced using the solvent peak. ^{19}F NMR are listed in parts per million downfield of $CFCl_3$ as an external standard. Coupling constants are given in hertz; routine couplings are not listed. Spectra were obtained at 25 °C in C_6D_6 unless otherwise noted. Magnetic susceptibility measurements were done by NMR using the Evans method[45] as modified by Sur,[46] with $(Me_3Si)_2O$ as an internal standard, or in the solid state using a SQUID magnetometer, as described below. Elemental analyses (C, H, N) were performed on a Perkin-Elmer 2400 CHN analyzer in our own laboratory, by Microlytics Analytical Laboratories of Deerfield, MA, or by Kolbe Microanalytical Laboratory, Mulheim an der Ruhr, Germany. X-ray data were collected on a Bruker SMART/CCD diffractometer; general experimental details are described in the literature.[47]

$[N_3N]MoCl$,[5] $[N_3N]Mo(N_2)$,[6] $[N_3N]WCl$, $[N_3N_F]MoCl$, $[N_3N_F]W(OTf)$, and $[N_3N_F]Mo(OTf)$[1] were synthesized as described in the literature, except $WCl_4(dme)$[48] was employed for the synthesis of the tungsten chloride. $[Cp_2Fe]OTf$[49] was prepared as described in the literature, while $[Cp_2Fe]BPh_4$ and $[Cp_2Fe]BAr^F_4$ were prepared in a manner analogous to the literature preparation of 1,1′-dimethylferrocenium tetraphenylborate.[50] $NaBAr^F_4$ was prepared by the method of Brookhart.[51] $V(Mes)_3(THF)$ was prepared as described by Seidel and Kreisel.[24] Sodium amalgam (0.5 wt %) was freshly prepared from sodium spheres and triply distilled mercury (Strem). CO (99.99%) and ethylene (polymer grade) were purchased from Matheson and used directly from the cylinder. ^{13}CO was purchased from Cambridge Isotope Laboratories. Other reagents were purchased from commercial vendors and used as received.

SQUID Magnetic Susceptibility Measurements. Measurements were carried out on a Quantum Design SQUID magnetometer. Data were obtained at a field strength of 5000 G. Straws and gel caps (Gelatin Capsule No. 4 Clear) were purchased from Quantum Design. The sample was prepared in the drybox by the following method. A gel cap and a square of Parafilm were weighed. The sample was placed in the gel cap and the Parafilm inserted above it. The gel cap was closed, and the mass of the sample was ascertained by weighing the loaded gel cap. The gel cap was placed in a straw, which was then mounted on the sample rod and placed in the magnetometer. Two runs were performed on the sample, one from 5 to 300 K and a second from 300 to 5 K. Measurements were made at the following increments: 5−10 K (every 1 K), 10−20 K (every 2 K), 20−50 K (every 3 K), 50−100 K (every 5 K), 100−200 K (every 10 K), 200−300 K (every 20 K).

$[N_3N]Mo(CO)$. $[N_3N]Mo(N_2)$ (100 mg, 0.21 mmol) was dissolved in 5 mL of benzene and sealed in a 25 mL bomb. The solution was subjected to two freeze−pump−thaw cycles, and 1 equiv of carbon monoxide was introduced. Over 15 min the solution changed color from orange-red to emerald green. After 3 h the solvent was removed in vacuo and the residue extracted with 5 mL of pentane. The pentane solution was cooled to −20 °C to give the product as green needles: yield 85 mg (85%); ^{1}H NMR δ 13.17 (CH_2), −2.03 ($SiMe_3$), −38.04 (CH_2); IR (Nujol) cm^{-1} 1841, 1832 (ν_{CO}); IR (pentane) cm^{-1} 1859 (ν_{CO}); μ = 1.77 μ_B (SQUID). Anal. Calcd for $C_{16}H_{39}N_4Si_3MoO$: C, 39.73; H, 8.13; N, 11.58. Found: C, 39.54; H, 8.18; N, 11.55.

$[N_3N]Mo{\equiv}COSiMe_3$. $[N_3N]Mo(CO)$ (100 mg, 0.21 mmol) was dissolved in 5 mL of THF. Magnesium powder (20 mg, 0.87 mmol) and TMSCl (45 μL, 0.36 mmol) were added, and the mixture was stirred for 3.5 h. The solvent was removed in vacuo and the residue extracted with 7 mL of pentane. The pentane solution was filtered through a pad of Celite, and the volume was reduced to 3 mL. The pentane solution was cooled to −20 °C to give the product as pale yellow needles: yield 105 mg (91%); ^{1}H NMR δ 3.48 (t, NCH_2CH_2N), 3.24 (t, NCH_2CH_2N), 0.49 (s, $SiMe_3$), 0.40 (s, $SiMe_3$); ^{13}C NMR δ 208.34 (Mo*C*OSiMe$_3$), 53.53 (NCH_2CH_2N), 52.56 (NCH_2CH_2N), 5.07 ($SiMe_3$), 2.55 ($SiMe_3$). Anal. Calcd for $C_{19}H_{48}N_4Si_4MoO$: C, 40.98; H, 8.69; N, 10.06. Found: C, 40.69; H, 8.70; N, 10.07.

$[N_3N]Mo(CN\text{-}t\text{-}Bu)$. $[N_3N]Mo(N_2)$ (150 mg, 0.31 mmol) was dissolved in 5 mL of toluene, and the solution was cooled to −20 °C. t-BuNC (39 mg, 0.47 mmol) was added to the solution, which was stirred overnight. The solvent was removed in vacuo to give an orange residue. The product was obtained as rust-colored needles upon recrystallization of the crude product from diethyl ether: yield 160 mg (96%); ^{1}H NMR δ 13.37 (CH_2), 3.76 (t-Bu), 0.12 ($SiMe_3$), −39.00 (CH_2); IR (Nujol) cm^{-1} 1838 (br, ν_{NC}); μ = 1.74 μ_B (SQUID).

$[N_3N]Mo(CNAr)$. $[N_3N]Mo(N_2)$ (75 mg, 0.16 mmol) was dissolved in 4 mL of toluene, and the solution was cooled to −20 °C. 2,6-$Me_2C_6H_3NC$ (25 mg, 0.19 mmol) was dissolved in 1 mL of toluene and the solution added to the stirred solution of $[N_3N]Mo(N_2)$. After 1 h the toluene was removed in vacuo and the residue was extracted with 7 mL of hexamethyldisiloxane. After filtering, the solution was cooled to −20 °C to afford the product as red plates: yield 56 mg (62%, not optimized); ^{1}H NMR δ 61.90 (NCH_2CH_2N, $\Delta\nu_{1/2}$ = 509 Hz), 37.15 (Ar H, $\Delta\nu_{1/2}$ = 138 Hz), 1.87 ($SiMe_3$, $\Delta\nu_{1/2}$ = 47 Hz), −0.66 (CH_3, $\Delta\nu_{1/2}$ = 156 Hz), −29.81 (NCH_2CH_2N, $\Delta\nu_{1/2}$ = 276 Hz), −68.85 (Ar H, $\Delta\nu_{1/2}$ = 882 Hz); IR (Nujol) cm^{-1} 1740 (ν_{NC}). Anal. Calcd for $C_{24}H_{48}N_5Si_3Mo$: C, 49.12; H, 8.24; N, 11.93. Found: C, 48.93; H, 8.31; N, 11.82.

{$[N_3N]Mo(CN\text{-}t\text{-}Bu)$}OTf. $[N_3N]Mo(CN\text{-}t\text{-}Bu)$ (110 mg, 0.20 mmol) was dissolved in 4 mL of THF, and the solution was cooled to −20 °C. $[FeCp_2]OTf$ (68 mg, 0.20 mmol) was added to the solution, and the reaction mixture was stirred for 25 min. The solvent was removed in vacuo, and the residue was washed with 20 mL of pentane in order to remove ferrocene. The residue was dried to give the product as a burnt-orange powder: yield 129 mg (92%); ^{1}H NMR (THF-d_8) δ 12.83 ($SiMe_3$), 9.28 (t-Bu), −29.38 (CH_2), −98.14 (CH_2); ^{19}F NMR (THF-d_8) δ −78.64 (CF_3SO_3); IR (THF) cm^{-1} 2147 (ν_{NC}); μ = 2.71 μ_B (SQUID).

$[N_3N]Mo(CN)$. $[N_3N]Mo(CN\text{-}t\text{-}Bu)$ (65 mg, 0.12 mmol) was dissolved in 6 mL of toluene. The solution was sealed in a low-pressure glass bomb and was heated to 86 °C for 36 h, during which time the color changed from orange to yellow. The solvent was removed, and the yellow solid was washed with cold pentane: yield 51 mg (88%); ^{1}H NMR δ 7.73 ($SiMe_3$), −25.7 (CH_2), −112.4 (CH_2); μ = 2.73 μ_B (SQUID). Anal. Calcd for $C_{16}H_{39}N_5Si_3Mo$: C, 39.89; H, 8.16; N, 14.54. Found: C, 39.72; H, 8.31; N, 14.55.

$[N_3N]Mo(C_2H_4)$. $[N_3N]MoCl$ (650 mg, 1.32 mmol) was dissolved in 15 mL of THF, and the solution was placed in a glass bomb with a stirring bar and magnesium powder (64 mg, 2.67 mmol). The vessel was sealed and subjected to three freeze−pump−thaw cycles in order to remove any dinitrogen present. Ethylene (~5 equiv) was condensed onto the frozen solution. The solution was thawed and stirred for 12 h, during which time the color changed from orange-red to purple. The solvent was removed in vacuo, and the residue was extracted with 20 mL of pentane. The extract was filtered through Celite and the pentane was removed from the filtrate in vacuo. The purple solid was recrystallized from hexamethyldisiloxane at −20 °C to afford the product as purple needles: yield 623 mg

(45) Evans, D. F. *Chem. Commun.* **1959**, 2003.
(46) Sur, S. K. *J. Magn. Reson.* **1989**, *82*, 169.
(47) Rosenberger, C.; Schrock, R. R.; Davis, W. M. *Inorg. Chem.* **1997**, *36*, 123.
(48) Persson, C.; Andersson, C. *Inorg. Chim. Acta* **1993**, *203*, 235.
(49) Schrock, R. R.; Sturgeoff, L. G.; Sharp, P. R. *Inorg. Chem.* **1983**, *22*, 2801.
(50) Jordan, R. F.; LaPointe, R. E.; Bradley, P. K.; Baezinger, N. *Organometallics* **1989**, *8*, 2892.
(51) Brookhart, M.; Grant, B.; Volpe, A. F. *Organometallics* **1992**, *11*, 3920.

(97%); ^{1}H NMR δ 3.63 ($SiMe_3$); μ = 1.73 μ_B (SQUID). Anal. Calcd for $C_{17}H_{43}N_4Si_3Mo$: C, 42.21; H, 8.96; N, 11.58. Found: C, 42.39; H, 9.31; N, 11.55.

[N_3N_F]Mo(CO)Na(15-crown-5). A two-chamber reaction vessel was charged with 0.5% Na/Hg (7 g, 1.5 mmol Na) in one chamber, and a suspension of [N_3N_F]Mo(OTf) (443 mg, 0.5 mmol) in THF (10 mL) in the other chamber. The vessel was degassed via three freeze−pump−thaw cycles and refilled with CO (400 mmHg, 2 mmol). The reaction mixture was stirred for 2 h, during which time all of the insoluble triflate dissolved to yield an orange solution. The vessel was pumped back into the drybox, and the reaction mixture was decanted from the excess amalgam. A solution of 15-crown-5 (132 mg, 0.6 mmol) in 2 mL of THF was added. The mixture was stirred for 1 h, the THF was removed, and the residue was dissolved in toluene. The salts were filtered off, and the toluene solution was concentrated to 1 mL. Pentane (0.5 mL) was added, and the solution was cooled to −40 °C overnight to yield orange crystals. The mother liquor was decanted off, and the crystals were washed three times with pentane: yield 328 mg (0.325 mmol, 65%); ^{1}H NMR δ 3.73 (t, 6, CH_2), 3.19 (s, 20, crown), 2.22 (t, 6, CH_2); ^{13}C NMR δ 226.69 (CO), 143.50 (d, C_o, J_{CF} = 240), 140.32 (br s, C_{ipso}), 138.20 (d, C_m, J_{CF} = 245), 135.40 (d, C_p, J_{CF} = 231), 70.21 (crown), 56.46 (CH_2), 53.27 (CH_2); ^{19}F NMR δ −151.73 (d, 6, F_o), −168.81 (t, 6, F_m), −174.56 (t, 3, F_p); IR (Nujol) 1701 cm^{-1} (ν_{CO}). Anal. Calcd for $C_{35}H_{32}F_{15}N_4O_6$NaMo: C, 41.68; H, 3.20; N, 5.56. Found: C, 41.55; H, 3.21; N, 5.43.

[N_3N_F]Mo≡COSiMe$_3$. A two-chamber reaction vessel was charged with [N_3N_F]W(OTf) (443 mg, 0.5 mmol) and THF (8 mL) in one chamber and 0.5% Na/Hg (5.75 g, 1.25 mmol. Na) in the other. The vessel was degassed by performing three freeze−pump−thaw cycles and refilled with CO (400 mmHg, 2 mmol). The reaction mixture was thawed and stirred for 2 h to yield a dark orange solution. The vessel was pumped back into the drybox, and the reaction mixture was decanted from the excess amalgam. A solution of chlorotrimethylsilane (82 mg, 0.75 mmol) in THF (2 mL) was added to the reaction mixture, resulting in a color change to pale yellow and the precipitation of a white powder. THF was removed, and the residue was dissolved in ether. The salts were filtered off, and the ether solution was cooled to −40 °C. Colorless crystals (211 mg, 0.25 mmol, 50%) were collected in two crops: ^{1}H NMR δ 3.37 (t, 6, CH_2), 2.13 (t, 6, CH_2), −0.49 (s, 9, $SiMe_3$); ^{13}C NMR δ 212.44 (CO), 142.81 (d, C_o, J_{CF} = 244), 137.97 (br s, C_{ipso}), 137.93 (d, C_m, J_{CF} = 248), 137.09 (d, C_p, J_{CF} = 246), 57.34 (CH_2), 52.78 (CH_2), −1.61 ($SiMe_3$); ^{19}F NMR δ −150.40 (d, 6, F_o), −165.23 (t, 6, F_m), −165.91 (t, 3, F_p). Anal. Calcd for $C_{28}H_{21}F_{15}N_4$OSiMo: C, 40.11; H, 2.52; N, 6.68. Found: C, 39.87; H, 2.58; N, 6.75.

[N_3N_F]Mo(CO). A solution of [N_3N_F]Mo(CO)Na(15-crown-5) (252 mg, 0.25 mmol) in THF (6 mL) was cooled to −40 °C. Ferrocenium tetraphenylborate (126 mg, 0.25 mmol) was added as a solid, and the color of the reaction mixture immediately changed from orange to green. After the mixture was stirred for 1 h at room temperature, THF was removed, and the residue was dissolved in ether. Sodium tetraphenylborate was removed by filtration. The ether was removed in vacuo, and the residue was washed several times with pentane to remove ferrocene and yield 158 mg (0.206 mmol, 83%) of spectroscopically pure green powder. Analytically pure material was obtained by recrystallization from a mixture of ether and pentane at −40 °C: ^{1}H NMR δ 12.85 (br s, CH_2), −23.90 (br s, CH_2); ^{19}F NMR δ −126.8 (br s, F_m), −167.00 (s, F_p); IR (Nujol) cm^{-1} 1889 (ν_{CO}); μ_{eff} = 2.1 μ_B (Evans method). Anal. Calcd for $C_{25}H_{12}F_{15}N_4$OMo: C, 39.24; H, 1.58; N, 7.32. Found: C, 39.16; H, 1.65; N, 7.26.

[N_3N_F]W(CO). A 100 mL round-bottomed flask was charged with [N_3N_F]W(OTf) (500 mg, 0.513 mmol), 25 mL of THF, 0.5% Na/Hg amalgam (2.36 g, 0.513 mmol, 1 equiv), and a stir bar. The flask was fitted with a vacuum adapter and attached to a high-vacuum line. It was degassed three times by a freeze−pump−thaw cycle, and CO (2.05 mmol, 4 equiv) was introduced by vacuum transfer at 77 K. The reaction flask was then sealed and warmed to room temperature, and the solution was stirred for 2.5 h. The volatile components were removed in vacuo, and the red residue was extracted with dichloromethane. The solution was filtered through Celite and the volume reduced to ∼ 4 mL. Pentane (10 mL) was layered on top of the dichloromethane solution, and the sample was stored at −40 °C for 3 days. The red crystalline product was isolated by decanting off the mother liquor: yield 330 mg in two crops (76%); ^{1}H NMR δ 29.3 (br s, $\Delta_{1/2}$ = 553, NCH_2N), −19.2 (br s, $\Delta_{1/2}$ = 415, NCH_2N); ^{19}F NMR δ −132.1 (br s, $\Delta_{1/2}$ = 277), −170.5 (s); IR (Nujol) cm^{-1} 1846 (ν_{CO}); μ_{eff} = 2.6 μ_B (Evans method). Anal. Calcd for $C_{25}H_{12}N_4F_{15}$OW: C, 35.19; H, 1.42; N, 6.57. Found: C, 35.45; H, 1.45; N, 6.74.

Observation of {[N_3N_F]W(CO)$_2$}NaL$_3$ (L = THF, Ether). A 50 mL Schlenk flask was charged with 0.5% Na/Hg (5.75 g, 1.25 mmol Na), [N_3N_F]W(OTf) (487 mg, 0.5 mmol), and 15 mL of THF. The vessel was degassed by performing three freeze−pump−thaw cycles and refilled with CO (300 mmHg, 1.75 mmol). When the reaction mixture was thawed to room temperature, the color turned deep purple immediately, and all of the insoluble triflate dissolved. ^{19}F NMR (THF) δ −151.43 (br s, 2, F_o), −151.68 (br s, 4, F_o), −170.17 (t, 4, F_m), −171.05 (t, 2, F_m), −175.60 (t, 2, F_p), −177.18 (t, 1, F_p); ^{13}C NMR (THF) δ 246.24 (t, ^{13}CO, J_{WC} = 112), 242.39 (t, ^{13}CONa, J_{WC} = 215); IR (Nujol) cm^{-1} 1926 (CO), 1716 (CONa); IR (THF) cm^{-1} 1952 (ν_{CO}), 1726 (ν_{CONa}); 1895 (ν^{13}_{CO}), 1682 (ν^{13}_{CONa}). ^{13}C-labeled material was prepared in an analogous fashion using ^{13}CO. The reaction can also be performed in ether. When an ether solution was stored for several months at −40 °C, crystals were obtained that were suitable for an X-ray diffraction study.

[N_3N_F]W(CO)Na(15-crown-5). Purple {[N_3N_F]W(CO)$_2$}Na(THF)$_3$ was prepared as described above from 292 mg of [N_3N_F]W(OTf) (0.3 mmol) and 3.45 g of Na/Hg (0.75 mmol). Prolonged exposure of the THF solution to vacuum left a yellow solid. The yellow solid was dissolved in toluene, and a solution of 15-crown-5 (79 mg, 0.36 mmol) was added, which resulted in precipitation of more sodium salts and a darkening of the solution from yellow to orange. After 30 min, the reaction was filtered through Celite, and the solution was concentrated to 2 mL. Adding an equal volume of pentane and cooling the mixture to −40 °C resulted in the formation of orange crystals. The mother liquor was decanted off, and the crystals were obtained: yield 194 mg (0.177 mmol, 59%); ^{1}H NMR δ 3.63 (t, 6, CH_2), 2.86 (s, 20, crown), 2.20 (t, 6, CH_2); ^{13}C NMR (THF) δ 224.20 (t, ^{13}CO, J_{CW} = 270), 144.87, 142.97, 140.29, 138.63 (C_6F_5), 69.34 (crown), 57.55 (CH_2), 53.93 (CH_2); ^{19}F NMR δ -151.96 (d, 6, F_o), −168.89 (t, 6, F_m), −173.85 (t, 3, F_p); IR (Nujol) cm^{-1} 1628 (ν_{CO}), 1592 (ν^{13}_{CO}), 1564 ($\nu^{13}C^{18}O$). Anal. Calcd for $C_{35}H_{32}F_{15}N_4O_6$NaW: C, 38.34; H, 2.94; N, 5.11. Found: C, 38.21; H, 3.08; N, 4.96.

[N_3N_F]W≡COSiMe$_3$. A solution of [N_3N_F]W(CO) (100 mg, 0.117 mmol) in 5 mL of THF was added to 0.5% Na/Hg amalgam (539 mg, 0.117 mmol). The reaction mixture was stirred for 1 h, at which point ^{19}F NMR indicated clean formation of the anion. The reaction mixture was filtered, and trimethylsilyl chloride (18 μL, 0.14 mmol, 1.2 equiv) was added. The reaction mixture was stirred for 3 h, the volatile components were removed in vacuo, and the brown residue was extracted with dichloromethane. The solution was filtered through Celite and the volume reduced to ∼4 mL. Pentane (10 mL) was layered on top of the dichloromethane solution, and the sample was stored at −40 °C for 15 h. Brown blocks were isolated by decantation of the mother liquor: yield 73 mg (67%); ^{1}H NMR δ 3.33 (t, 6, NCH_2N), 2.10 (t, 6, NCH_2N), −0.487 (s, 9, $SiMe_3$); ^{19}F NMR δ −151.1 (s, 6, F_o), −165.7 (s, 9, F_m and F_p); ^{13}C NMR δ 216.9 (W≡*C*OSiMe$_3$), 144.8 (C_6F_5), 141.6 (C_6F_5), 139.3 (C_6F_5), 137.2 (C_6F_5), 136.0 (C_6F_5), 56.8 (NCH_2N), 52.1 (NCH_2N), −1.4 ($Si(CH_3)_3$). Anal. Calcd for

$C_{28}H_{21}N_4F_{15}OSiW$: C, 36.30; H, 2.28; N, 6.05. Found: C, 35.92; H, 2.18; N, 5.99.

$[N_3N_F]W(CO)V(Mes)_3$. $[N_3N_F]W(CO)$ (100 mg, 0.117 mmol) and V(mesityl)$_3$(THF) (56 mg, 0.12 mmol) were placed in a vial, and toluene (4 mL) was added. The deep black solution was stirred for 1 h, at which point ^{19}F NMR showed complete conversion to product. The reaction mixture was filtered and the volume of the toluene reduced to ~2 mL. Pentane was layered on and the vial cooled to −40 °C. After 15 h, black crystals had formed and were isolated by decanting the mother liquor: yield 130 mg in two crops (88%); ^1H NMR δ 17.5 (br s, $\Delta_{1/2}$ = 22, 9, mesityl Me_p), 16.2 (br s, $\Delta_{1/2}$ = 300, 18, mesityl Me_o), 6.6 (br s, $\Delta_{1/2}$ = 45, 6, mesityl H_m), 3.38 (s, 6, NCH_2N), 2.06 (s, 6, NCH_2N); ^{19}F NMR δ −153.2 (s, 6, F_o), −162.9 (s, 3, F_p), −164.3 (s, 6, F_m); IR (KBr) cm^{-1} 2916, 2867, 1587, 1501, 1278, 985, 851, 756, 729; μ_{eff} = 2.1 μ_B (Evans method). Anal. Calcd for $C_{59}H_{53}N_4F_{15}OVW$: C, 52.34; H, 3.95; N, 4.14. Found: C, 52.28; H, 3.77; N, 3.96.

$[N_3N_F]Mo(CN\text{-}t\text{-}Bu)$. A 50 mL round-bottom flask was charged with $[N_3N_F]Mo(OTf)$ (2.22 g, 2.5 mmol) and 0.5% Na/Hg (11.5 g, 2.5 mmol of Na). A solution of *tert*-butyl isocyanide (208 mg, 2.5 mmol) in THF (25 mL) was added, and the reaction mixture was stirred vigorously for 1 h. All of the $[N_3N_F]Mo(OTf)$ dissolved to give a red solution. THF was removed in vacuo, and the residue was redissolved in dichloromethane. Na(OTf) was removed by filtration, and crystals were grown from 10 mL of dichloromethane at −40 °C. Orange crystals were collected and dried in vacuo: yield 1.63 g (1.98 mmol, 79%); ^1H NMR δ 11.1 (br s, 9, t-Bu), 6.6 (br s, 6, CH_2), −28.2 (br s, 6, CH_2); ^{19}F NMR δ −59.8 (br s, 6, F_o), −143.6 (br s, 3, F_p), −159.7 (s, 6, F_m); IR (Nujol) cm^{-1} 1787 (ν_{NC}). Anal. Calcd for $C_{29}H_{21}F_{15}N_5Mo$: C, 42.46; H, 2.58; N, 8.54. Found: C, 42.40; H, 2.63; N, 8.44.

$[N_3N_F]W(CN\text{-}t\text{-}Bu)$. $[N_3N_F]WCl$ (700 mg, 0.813 mmol) and 0.5% Na/Hg amalgam (3.74 g, 0.813 mmol) were added to a 100 mL round-bottomed flask, and a solution of *tert*-butyl isocyanide (92 μL, 0.813 mmol) in 20 mL of THF was added. A ^{19}F NMR spectrum showed the reaction to be complete after 1 h. The solution was decanted from the amalgam, and the volatile components were removed in vacuo. The orange-brown residue was extracted with dichloromethane, and the extract was filtered through Celite. The volume was reduced until the solution was saturated (~20 mL), and the solution was then chilled to −40 °C overnight. Orange plates of the product were isolated by decantation: yield 683 mg in two crops (92%); ^1H NMR δ 13.6 (br s, $\Delta_{1/2}$ = 67, *t*-Bu), 8.0 (br s, $\Delta_{1/2}$ = 132, NCH_2N), −25.8 (br s, $\Delta_{1/2}$ = 99, NCH_2N); ^{19}F NMR δ −77.0 (br s, $\Delta_{1/2}$ = 86, F_o), −142.5 (s, F_m), −161.2 (s, F_p); IR (Nujol) cm^{-1} 1684 (ν_{NC}); μ_{eff} = 2.2 μ_B (Evans method); μ = 1.74(1) μ_B (SQUID). Anal. Calcd for $C_{29}H_{21}F_{15}N_5W$: C, 38.35; H, 2.33; N, 7.71. Found: C, 38.20; H, 2.22; N, 7.75.

$[N_3N_F]Mo(CNAr)$. This complex was synthesized in a manner similar to that used to prepare $[N_3N_F]Mo(CN\text{-}t\text{-}Bu)$, starting from $[N_3N_F]Mo(OTf)$ (900 mg, 1.015 mmol), 0.5% Na/Hg (4.67 g, 1.015 mmol Na), and a solution of 2,6-dimethylphenyl isocyanide (133 mg, 1.015 mmol) in THF (10 mL). Orange crystals (605 mg 0.70 mmol, 69%) were collected and dried in vacuo after crystallization from 4 mL of dichloromethane overnight at −40 °C: ^1H NMR δ 32.1 (br s, 2, H_m), 26.2 (br s, 6, CH_2), 6.4 (br s, 6, Ar Me), −22.7 (br s, 6, CH_2), −27.9 (br s, 1, H_p); ^{19}F NMR δ −72.0 (br s, 6, F_o), −141.3 (br s, 3, F_p), −160.5 (s, 6, F_m); IR (Nujol) cm^{-1} 1777 (ν_{NC}). Anal. Calcd for $C_{33}H_{21}F_{15}N_5Mo$: C, 45.64; H, 2.44; N, 8.06. Found: C, 45.72; H, 2.40; N, 8.01.

$[N_3N_F]W(CNAr)$. A 10 mL reaction vial was charged with $[N_3N_F]W(OTf)$ (714 mg, 0.73 mmol) and 0.5% Na/Hg (3.37 g, 0.73 mmol of Na). A solution of 2,6-dimethylphenyl isocyanide (96 mg, 0.73 mmol) in THF (10 mL) was added, and the reaction mixture was stirred vigorously for 1 h. All of the solid triflate dissolved to give a red solution. THF was removed in vacuo, and the residue was dissolved in dichloromethane. Na(OTf) was removed by filtration, and crystals were grown from dichloromethane at −40 °C. Orange crystals were collected and dried in vacuo: yield 573 mg (0.6 mmol, 82%); ^1H NMR δ 41.7 (br s, 2, meta), 31.8 (br s, 6, CH_2), 8.7 (br s, 6, Ar Me), −25.1 (br s, 6, CH_2), −33.1 (br s, 1, para); ^{19}F NMR δ −82.6 (br s, 6, F_o), −134.9 (br s, 3, F_p), −161.1 (s, 6, F_m); IR (Nujol) cm^{-1} 1679 (ν_{NC}). Anal. Calcd for $C_{33}H_{21}F_{15}N_5W$: C, 41.44; H, 2.21; N, 7.32. Found: C, 41.54; H, 2.34; N, 7.23.

$[N_3N_F]Mo(CN\text{-}n\text{-}Bu)$. $[N_3N_F]MoCl$ (200 mg, 0.259 mmol) and 0.5% sodium amalgam (1.19 g, 0.259 mmol) were added to a vial. A solution of *n*-butyl isocyanide (27 μL, 0.26 mmol) in 10 mL of THF was added all at once. The reaction mixture was stirred for 3 h, at which point ^{19}F NMR showed the reaction to be complete. This mixture was then filtered, and the volatile components were removed from the filtrate in vacuo. The product was recrystallized from dichloromethane by layering pentane on top and cooling the sample to −40 °C. After 15 h large reddish needles formed, which were isolated by decanting away the mother liquor: yield 162 mg (76%); ^1H NMR δ 5.7 (br s, $\Delta_{1/2}$ = 81, 6, NCH_2N), 5.2 (br s, $\Delta_{1/2}$ = 25, *n*-butyl), 4.0 (br s, $\Delta_{1/2}$ = 12, *n*-butyl), −0.1 (br s, $\Delta_{1/2}$ = 25, *n*-butyl), −27.6 (br s, $\Delta_{1/2}$ = 94, 6, NCH_2N); ^{19}F NMR δ −67 (br s, $\Delta_{1/2}$ = 716, 6, F_o), −144.0 (s, 3, F_p), −161.2 (s, 6, F_m); IR (Nujol) cm^{-1} 1790 (ν_{NC}); μ_{eff} = 2.3 μ_B (Evans method). Anal. Calcd for $C_{29}H_{21}N_5F_{15}Mo$: C, 42.46; H, 2.58; N, 8.54. Found: C, 42.14; H, 2.55; N, 8.53.

$\{[N_3N_F]W(CN\text{-}t\text{-}Bu)\}BAr^F{}_4$. A solution of $[N_3N_F]W(CN\text{-}t\text{-}Bu)$ (363 mg, 0.4 mmol) in CH_2Cl_2 (16 mL) was cooled to −40 °C. $[Cp_2Fe]BAr^F{}_4$ (420 mg, 0.4 mmol) was added as a solid, which resulted in an immediate color change from orange to red. The volume was reduced to 3 mL, and an equal volume of pentane was added. Red crystals were formed upon cooling to −40 °C for 2 h. The crystals were collected and dried in vacuo: yield 570 mg (0.32 mmol, 80%); ^1H NMR ($CDCl_3$) δ 7.38 (s, 4, $BAr^F{}_4$ para), 7.17 (s, 8, $BAr^F{}_4$ ortho), 0.70 (br s, 9, t-Bu), −28.1 (br s, 6, CH_2), −55.0 (br s, 6, CH_2); ^{19}F NMR ($CDCl_3$) δ −62.8 (s, 24, $BAr^F{}_4$) −98.6 (br s, 6, F_m), −148.3 (br s, 3, F_p); IR (Nujol) cm^{-1} 2136 (ν_{NC}); μ_{eff} = 2.8 μ_B (Evans method). Anal. Calcd for $C_{61}H_{33}BF_{39}N_5W$: C, 41.36; H, 1.88; N, 3.95. Found: C, 41.44; H, 1.90; N, 3.92.

$\{[N_3N_F]W(CN\text{-}t\text{-}Bu)\}BPh_4$. This complex was synthesized in a manner similar to that used to prepare $\{[N_3N_F]W(CN\text{-}t\text{-}Bu)\}BAr^F{}_4{}^-$, starting from $[N_3N_F]W(CN\text{-}t\text{-}Bu)$ (307 mg, 0.338 mmol) and $[Cp_2Fe]BPh_4$ (171 mg, 0.338 mmol). The red product (223 mg, 0.182 mmol, 54%) crystallized out of dichloromethane upon cooling the solution to −40 °C; IR (Nujol) cm^{-1} 2133 (ν_{NC}).

$\{[N_3N_F]W(CNAr)\}BAr^F{}_4$. This complex was synthesized in a manner similar to that used to prepare $\{[N_3N_F]W(CN\text{-}t\text{-}Bu)\}$-$BAr^F{}_4{}^-$, starting from $[N_3N_F]W(CNAr)$ (287 mg, 0.3 mmol) and $[Cp_2Fe]BAr^F{}_4$ (315 mg, 0.3 mmol), yielding 453 mg (0.25 mmol, 83%) of product as red crystals: ^1H NMR ($CDCl_3$) δ 46.51(s, 6, Ar Me), 41.12 (s, 2, meta), 7.39 (s, 4, $BAr^F{}_4$ para), 7.15 (s, 8, $BAr^F{}_4$ ortho), −27.8 (br s, 6, CH_2), −55.2 (br s, 6, CH_2), −70.56 (s, 1, para); ^{19}F NMR ($CDCl_3$) δ −62.8 (s, 24, $BAr^F{}_4$) −105.6 (br s, 6, F_m), −148.3 (br s, 3, F_p); IR (Nujol) cm^{-1} 2066 (ν_{NC}); μ_{eff} = 2.8 μ_B (Evans method). Anal. Calcd for $C_{65}H_{33}BF_{39}N_5W$: C, 42.91; H, 1.83; N, 3.85. Found: C, 43.04; H, 1.91; N, 3.96.

$\{[N_3N_F]Mo(CN\text{-}t\text{-}Bu)\}BAr^F{}_4$. This green crystalline complex was synthesized in a manner similar to that used to prepare $\{[N_3N_F]W(CN\text{-}t\text{-}Bu)\}BAr^F{}_4$, starting from $[N_3N_F]Mo$-$(CN\text{-}t\text{-}Bu)$ (328 mg, 0.4 mmol) and $[FeCp_2]BAr^F{}_4$ (420 mg, 0.4 mmol): yield 591 mg (0.35 mmol, 88%). No pentane was required for crystallization: ^1H NMR ($CDCl_3$) δ 7.8 (br s, t-Bu), 7.61 (s, 4, $BAr^F{}_4$ H_o), 7.48 (s, 8, $BAr^F{}_4$ H_p), −20.2 (br s, 6, CH_2), −80.7 (br s, 6, CH_2); ^{19}F NMR ($CDCl_3$) δ −63.1 (s, $BAr^F{}_4$) −82.5 (br s, F_m), −154.5 (br s, F_p); IR (Nujol) cm^{-1} 2184 (ν_{NC}); μ_{eff} = 3.1 μ_B (Evans method). Anal. Calcd for $C_{61}H_{33}BF_{39}N_5Mo$: C, 43.52; H, 1.98; N, 4.16. Found: C, 43.38; H, 2.08; N, 3.90.

$\{[N_3N_F]Mo(CNAr)\}BAr^F{}_4\cdot CH_2Cl_2$. This complex was synthesized in a manner similar to that used to prepare $[N_3N_F]$-$Mo(CN\text{-}t\text{-}Bu)\}BAr^F{}_4$, starting from $[N_3N_F]Mo(CNAr)$ (304 mg,

0.35 mmol) and $[FeCp_2]BAr^F_4$ (367 mg, 0.35 mmol): yield 513 mg (0.28 mmol, 81%) of green crystals. The product crystallizes immediately upon formation, and 1 equiv of dichloromethane is present in the lattice: ^{1}H NMR ($CDCl_3$) δ 38.8 (s, 6, Ar Me), 36.9 (s, 2, H_m), 7.68 (s, 8, BAr^F_4 H_o), 7.56 (s, 4, BAr^F_4 H_p), 5.30 (CH_2Cl_2), −21.0 (br s, 6, CH_2), −44.01 (s, 1, H_p), −81.2 (br s, 6, CH_2); ^{19}F NMR ($CDCl_3$) δ −62.7 (s, 24, BAr^F_4) −89.1 (br s, 6, F_m), −150.3 (br s, 3, F_p); IR (Nujol) cm^{-1} 2133 (ν_{NC}); μ_{eff} = 3.3 μ_B (Evans method). Anal. Calcd for $C_{66}H_{35}BCl_2F_{39}N_5Mo$: C, 43.64; H, 1.94; N, 3.86. Found: C, 43.67; H, 2.06; N, 3.79.

{[N_3N_F]W(CN-t-Bu)$_2$}OTf. (a) From [N_3N_F]W(CN-t-Bu). A solution of [N_3N_F]W(CN-t-Bu) (136 mg, 0.15 mmol, in THF (5 mL)) was cooled to −40 °C. Ferrocenium triflate (50 mg, 0.15 mmol) was added as a solid, and the reaction mixture was warmed to room temperature with stirring. The color turned from orange to deep red as soon as the $[FeCp_2]$OTf dissolved. Within 5 min, yellow solid [N_3N_F]W(OTf) began to precipitate out. [N_3N_F]W(OTf) (68 mg, 0.07 mmol, 47%) of triflate was collected by filtration. The mother liquor was concentrated to dryness and extracted with ether in order to remove ferrocene. The insoluble product (78 mg, 0.074 mmol, 49%) was collected and washed several times with ether: ^{1}H NMR ($CDCl_3$) δ 4.09 (t, 6, CH_2), 3.76 (t, 6, CH_2), 1.09 (s, 18, t-Bu); ^{13}C NMR ($CDCl_3$) δ 157.33 (WC≡N), 144.02 (C_6F_5), 142.11 (C_6F_5) 140.34 (C_6F_5), 138.48 (C_6F_5), 134.96 (C_6F_5), 63.71 (CH_2), 59.88 (t-BuC), 53.93 (CH_2), 30.22 (t-BuMe); ^{19}F NMR ($CDCl_3$) δ −78.80 (s, 3, OTf), −147.93 (s, 6, F_o), −158.68 (t, 3, F_p), −162.09 (s, 6, F_m); IR (Nujol) cm^{-1} 2111 and 2104 (ν_{NC}). Anal. Calcd for $C_{35}H_{30}F_{18}N_6O_3SW$: C, 36.86; H, 2.65; N, 7.37. Found: C, 37.08; H, 2.78; N, 7.46.

(b) From [N_3N_F]W(OTf) and *tert*-Butyl Isocyanide. [N_3N_F]W(OTf) (779 mg, 0.8 mmol) was added slowly as a solid to a solution of *tert*-butyl isocyanide (140 mg, 1.68 mmol) in THF (10 mL). The solution initially turned green, but it became dark orange upon addition of all of the isocyanide. The reaction was stirred for 30 min before THF was removed in vacuo. The residue was extracted with ether, and the insoluble product (801 mg, 0.702 mmol, 88%) was collected, washed with ether, and dried in vacuo.

{[N_3N_F]W(CNAr)$_2$}OTf. [N_3N_F]W(OTf) (779 mg, 0.8 mmol) was added as a solid to a solution of 2,6-dimethylphenyl isocyanide (210 mg, 1.6 mmol) in THF (8 mL). The solution turned red, and all of the triflate dissolved. After 30 min, pentane (4 mL) was added in order to precipitate the product as a green powder (817 mg, 0.66 mmol, 83%), which was collected, washed with ether and pentane, and dried in vacuo: ^{1}H NMR ($CDCl_3$) δ 7.20 (t, 2, H_p), 7.07 (d, 4, H_m), 4.18 (s, 6, CH_2), 3.92 (s, 6, CH_2), 2.12 (br s, 12, Me_o); ^{13}C NMR ($CDCl_3$) δ 174.70 (WC≡N), 142.45 (d, C_o, J_{CF} = 251), 138.97 (d, C_p, J_{CF} = 257), 137.28 (d, C_m, J_{CF} = 257), 134.50 (br s, C_{ipso}), 134.62 (Ar), 130.75 (Ar), 128.47 (Ar), 125.73 (Ar), 62.96 (CH_2), 54.20 (CH_2), 17.42 ($ArCH_3$); ^{19}F NMR ($CDCl_3$) δ −78.81 (s, 3, OTf), −146.88 (s, 6, F_o), −158.31 (t, 3, F_p), −162.53 (s, 6, F_m); IR (Nujol) cm^{-1} 2096, 2058 (ν_{NC}). Anal. Calcd for $C_{43}H_{30}F_{18}N_6O_3SW$: C, 41.74; H, 2.45; N, 6.80. Found: C, 41.79; H, 2.36; N, 6.70.

{[N_3N_F]W(CNAr)$_2$}BAr$^F_4$. 2,6-Dimethylphenyl isocyanide (20 mg, 0.152 mmol) was added to a solution of {[N_3N_F]W(CNAr)}BAr^F_4 (182 mg, 0.1 mmol) in CH_2Cl_2 (4 mL). The color changed immediately from red to yellow. After removal of CH_2Cl_2, the residue was dissolved in ether. Addition of pentane resulted in the precipitation of the product as a yellow powder (153 mg, 0.078 mmol, 78%), which was collected, washed with pentane, and dried in vacuo: ^{1}H NMR ($CDCl_3$) δ 7.70 (br s, 8, BAr^F_4 ortho), 7.52 (br s, 4, BAr^F_4 para), 7.16 (t, 2, H_p), 7.05 (d, 4, H_m), 4.15 (s, 6, CH_2), 3.48 (s, 6, CH_2), 2.01 (br s, 12, Me_o); ^{19}F NMR ($CDCl_3$) δ −62.66 (s, 24, BAr^F_4), −146.90 (s, 6, F_o), −156.18 (t, 3, F_p), −160.95 (s, 6, F_m); IR (Nujol) cm^{-1} 2112, 2072 (ν_{NC}).

{[N_3N_F]Mo(CN-t-Bu)$_2$}OTf. This complex was synthesized in a manner similar to that used to prepare {[N_3N_F]W(CN-t-Bu)$_2$}OTf, starting from [N_3N_F]Mo(OTf) (443 mg, 0.5 mmol) and a solution of *tert*-butyl isocyanide (125 mg, 1.5 mmol) in THF (8 mL). No color changes were observed during the course of reaction. The orange product (303 mg, 0.28 mmol, 57%) was collected, washed with ether, and dried in vacuo: ^{1}H NMR ($CDCl_3$, 0 °C) δ 4.06 (br s, 6, CH_2), 3.65 (br s, 6, CH_2), 1.15 (br s, 18, t-Bu); ^{13}C NMR ($CDCl_3$) δ 144.57 (C_6F_5), 142.67 (C_6F_5), 138.19 (C_6F_5), 136.17 (C_6F_5), 58.45 (CH_2), 56.76 (CH_2), 30.71 (t-Bu), 29.67 (t-Bu); ^{19}F NMR ($CDCl_3$) δ −78.80 (s, 3, OTf), −147.98 (br s, 6, F_o), −159.07 (br s, 3, F_p), −162.92 (br s, 6, F_m). IR (Nujol) cm^{-1} 2162, 2136 (ν_{NC}). Anal. Calcd for $C_{35}H_{30}F_{18}N_6O_3SMo$: C, 39.94; H, 2.87; N, 7.98. Found: C, 39.83; H, 2.94; N, 7.99.

{[N_3N_F]Mo(CNAr)$_2$}OTf. This complex was synthesized in a manner similar to that used to prepare {[N_3N_F]W(CNAr)$_2$}OTf, starting from [N_3N_F]Mo(OTf) (709 mg, 0.8 mmol) and 2,6-dimethylphenyl isocyanide (315 mg, 2.4 mmol). The product (589 mg, 0.51 mmol, 64%) was isolated as a yellow powder. ^{1}H NMR ($CDCl_3$, 0 °C) δ 7.16 (t, 2, H_p), 7.05 (d, 4, H_m), 4.28 (s, 6, CH_2), 3.97 (s, 6, CH_2), 2.01 (s, 12, Me_o); ^{13}C NMR ($CDCl_3$) δ 172.38 (MoC≡N), 141.83 (d, C_o, J_{CF} = 249), 138.53 (d, C_p, J_{CF} = 255), 137.32 (d, C_m, J_{CF} = 253), 134.89 (br s, C_{ipso}), 134.28 (Ar), 131.09 (Ar), 128.58 (Ar), 124.96 (Ar), 63.36 (CH_2), 54.28 (CH_2), 17.49 ($ArCH_3$); ^{19}F NMR ($CDCl_3$) δ −78.86 (s, 3, OTf), −147.28 (s, 6, F_o), −158.24 (t, 3, F_p), −162.44 (s, 6, F_m); IR (Nujol) cm^{-1} 2116, 2095 (ν_{NC}). Anal. Calcd for $C_{43}H_{30}F_{18}N_6O_3SMo$: C, 44.96; H, 2.63; N, 7.32. Found: C, 45.11; H, 2.57; N, 7.21.

{[N_3N_F]W(CN-t-Bu)$_3$}OTf. [N_3N_F]W(OTf) (390 mg, 0.4 mmol) was added as a solid to a stirred solution of *tert*-butyl isocyanide (133 mg, 1.6 mmol) in THF (5 mL). The reaction mixture turned green immediately, and all triflate dissolved within 5 min. The mixture was stirred for 15 min, and 3 mL of pentane was added in order to precipitate the lime green product, which was collected, washed with ether and pentane, and dried in vacuo: yield 421 mg (0.34 mmol, 86%). Analytically pure material was obtained by recrystallization from dichloromethane and pentane in the presence of excess isocyanide: ^{1}H NMR ($CDCl_3$, −20 °C, 500 MHz) δ 4.21 (s, 2), 4.08 (m, 2), 3.89 (m, 2), 3.54 (m, 4), 3.27 (s, 2), 1.68 (s, 9, t-Bu), 1.07 (s, 18, t-Bu); ^{13}C NMR ($CDCl_3$) δ 150.49 (WC≡N), 146.04 (C_6F_5), 144.41 (C_6F_5), 144.14 (C_6F_5), 142.45 (C_6F_5), 140.32 (C_6F_5), 139.20 (C_6F_5), 138.27 (C_6F_5), 137.02 (C_6F_5), 135.44 (C_6F_5), 68.70 (CH_2), 64.45 (CH_2), 60.11 (CH_2), 59.23 (CH_2), 59.06 (CH_2), 58.19 (CH_2), 31.41 (t-Bu), 30.49 (t-Bu); ^{19}F NMR (THF, 470 MHz) δ −78.80 (s, 3, (OTf)), −145.58 (br s, 2, F_o), −145.82 (br s, 2, F_o), −147.76 (br s, 2, F_o), −163.25 (t, 2, F_m), −165.03 (t, 4, F_m), −166.30 (t, 2, F_p), −167.47 (t, 1, F_p); ^{19}F NMR ($CDCl_3$) δ −146.38 (br s, 2, F_o), −147.53 (d, 2, F_o), −148.90 (br s, 2, F_o), −161.39 (t, 2, F_m), −163.49 (t, 2, F_m), −164.23 (t, 2, F_m), −165.52 (br s, 3, F_p); IR (Nujol) cm^{-1} 2178, 2145 (ν_{NC}). Anal. Calcd for $C_{40}H_{39}F_{18}N_7O_3SW$: C, 39.26; H, 3.21; N, 8.01. Found: C, 39.06; H, 3.29; N, 7.88.

{[N_3N_F]W(CN-t-Bu)$_3$}BPh$_4$. A solution of *tert*-butyl isocyanide (37 mg, 0.45 mmol) in THF (4 mL) was added to solid {[N_3N_F]W(CN-t-Bu)}BPh_4 (184 mg, 0.15 mmol), which dissolved as it reacted to give a green solution. The solution was cooled to −40 °C, which resulted in the crystallization of green product (210 mg, 0.15 mmol, 100%); ^{1}H NMR ($CDCl_3$, −3 °C, 500 MHz) δ 7.36 (br s, 8, BPh_4 ortho), 7.01 (t, 8, BPh_4 meta), 6.87 (t, 4, BPh_4 para), 4.04 (s, 2), 3.66 (m, 2), 3.10 (m, 2), 2.88 (m, 2), 2.78 (br s, 4), 1.62 (s, 9, t-Bu), 1.00 (s, 18, t-Bu); ^{19}F NMR (THF) δ −144.94 (br s, 2, F_o), −145.85 (d, 2, F_o), −147.47 (br s, 2, F_o), −162.22 (t, 2, F_m), −164.10 (t, 2, F_m), −164.38 (t, 2, F_m), −165.60 (t, 2, F_p), −166.44 (t, 1, F_p); ^{19}F NMR ($CDCl_3$) δ −144.41 (br s, 2, F_o), −146.17 (d, 2, F_o), −147.24 (br s, 2, F_o), −159.45 (t, 2, F_m), −161.51 (t, 2, F_m), −162.38 (t, 2, F_m), −163.59 (br s, 3, F_p); IR (Nujol) cm^{-1} 2175, 2140 (ν_{NC}).

[N_3N_F]W(C_2H_4). A 100 mL round-bottomed flask was charged with [N_3N_F]W(OTf) (500 mg, 0.513 mmol), sodium amalgam (2.60 g, 0.564 mmol of Na), and THF (50 mL). It was

fitted with a vacuum adapter, sealed, and attached to a high-vacuum line. After degassing by freeze−pump−thawing, ethylene (~40 mmol) was introduced by vacuum transfer. The reaction vessel was sealed, and the contents were warmed to room temperature and stirred for 1 h. The solution was decanted off the amalgam, filtered, concentrated to dryness, and extracted with CH_2Cl_2. The brown product was recrystallized from dichloromethane by layering a concentrated solution with pentane and storing the sample at −40 °C for 15 h: yield 346 mg (79%) in two crops; ^{19}F NMR δ −100 (v br s, $\Delta_{1/2}$ = 2,500, 6, F_o), −137 (br s, $\Delta_{1/2}$ = 650, 6, F_m), −152.1 (br s, $\Delta_{1/2}$ = 140, 3, F_p); μ_{eff} = 1.8 μ_B (Evans method). Anal. Calcd for $C_{26}H_{16}N_4F_{15}W$: C, 36.60; H, 1.89; N, 6.57. Found: C, 36.54; H, 2.03; N, 6.36.

{[N_3N_F]W(C_2H_4)}OTf. Ferrocenium triflate (83 mg, 0.23 mmol) was added as a solid to a solution of [N_3NF]W(C_2H_4) (200 mg, 0.234 mmol) in 8 mL of THF. The solution turned deep red instantly. After 15 min, the solution was filtered and the THF was removed in vacuo. The ferrocene was sublimed away from the product onto a −78 °C probe. The solid which remained was recrystallized from dichloromethane by addition of pentane to give the product as a red solid: yield 215 mg (91%); ^{1}H NMR δ 4.42 (br s, 6, NCH_2CH_2N), 3.96 (br s, 6, NCH_2CH_2N), 3.10 (s, 4, C_2H_4); ^{19}F NMR ($CDCl_3$) δ −78 (br s, 3, (OTf)), −143.7 (s, 6, F_o), −152.7 (s, 3, F_p), −159.8 (s, 6, F_m). Anal. Calcd for $C_{27}H_{16}N_4F_{18}O_3SW$: C, 32.35; H, 1.61; N, 5.59. Found: C, 32.53; H, 1.63; N, 5.46.

X-ray Structure of [N_3N]Mo(CN). A yellow crystal was mounted in oil and placed in a cold stream of nitrogen attached to a Bruker SMART/CCD diffractometer. A total of 11 177 reflections were collected, of which 2052 were determined to be unique. Integration of greater than a half-hemisphere of data using the SAINT program revealed tetragonal Laue symmetry. Systematic absences indicated $P\bar{4}2_1m$ as the space group. Solution (direct methods) and refinement of the structure was performed with the ShelXTL set of programs. All non-hydrogen atoms were refined anisotropically; hydrogen atoms were placed in idealized positions and refined using a riding model. A 0.5 equiv amount of ether was found in the unit cell. Crystallographic details are provided in Table 2 and selected interatomic distances and angles in Table 3.

X-ray Structure of {[N_3N_F]W($CO)_2$}Na(ether)$_3$. A purple crystal was mounted in oil and placed in a cold stream of nitrogen attached to a Bruker SMART/CCD diffractometer. A total of 9266 reflections were collected, of which 6264 were determined to be unique. An empirical absorption correction from ψ-scans was applied. Integration of greater than a half-hemisphere of data using the SAINT program revealed triclinic Laue symmetry and $P\bar{1}$ as the space group. Solution and refinement of the structure was performed with the ShelXTL set of programs. Patterson methods were employed to locate the tungsten atom, while subsequent difference Fourier calculations revealed the positions of the remaining non-hydrogen atoms. All non-hydrogen atoms were refined anisotropically; hydrogen atoms were placed in idealized positions and refined using a riding model. Disorder in one arm of one of the coordinated ether molecules was modeled over two positions. Crystallographic details are provided in Table 4 and selected interatomic distances and angles in Table 5.

X-ray Structure of [N_3N_F]W(CO)V(Mes)$_3$. A black crystal was mounted in oil and placed in a cold stream of nitrogen attached to a Bruker SMART/CCD diffractometer. A total of 15 746 reflections were collected, of which 5147 were determined to be unique. Integration of greater than a half-hemisphere of data using the SAINT program revealed monoclinic Laue symmetry. Systematic absences indicated $P2_1/c$ as the space group. Solution (direct methods) and refinement of the structure was performed with the ShelXTL set of programs. Only W, V, O, N, and F atoms were refined anisotropically; hydrogen atoms were placed in an idealized position and refined using a riding model. Crystallographic details are provided in Table 2 and selected interatomic distances and angles in Table 6.

X-ray Structure of [N_3N_F]W(CN-t-Bu). An orange crystal was mounted in oil and placed in a cold stream of nitrogen attached to a Bruker SMART/CCD diffractometer. A total of 9917 reflections were collected, of which 4215 were determined to be unique. Integration of greater than a half-hemisphere of data using the SAINT program revealed monoclinic Laue symmetry. Systematic absences indicated $P2_1/c$ as the space group. Solution (direct methods) and refinement of the structure was performed with ShelXTL set of programs. All non-hydrogen atoms were refined anisotropically; hydrogen atoms were placed in idealized positions and refined using a riding model. Crystallographic details are provided in Table 2 and selected interatomic distances and angles in Table 6.

X-ray Structure of {[N_3N_F]W(CN-t-Bu)$_3$}BPh$_4$. A green crystal was mounted in oil and placed in a cold stream of nitrogen attached to a Bruker SMART/CCD diffractometer. A total of 29 930 reflections were collected, of which 10 559 were determined to be unique. An empirical absorption correction from ψ-scans was applied. Integration of greater than a half-hemisphere of data using the SAINT program revealed monoclinic Laue symmetry. Systematic absences indicated $P2_1/c$ as the space group. Solution (direct methods) and refinement of the structure was performed with the ShelXTL set of programs. All non-hydrogen atoms were refined anisotropically; hydrogen atoms were placed in idealized positions and refined using a riding model. Three molecules of THF were found in the asymmetric unit. Crystallographic details are provided in Table 4 and selected interatomic distances and angles in Table 7.

Acknowledgment. R.R.S. is grateful to the National Institutes of Health (Grant No. GM 31978) for research support. G.E.G. thanks Pete Bonitatebus for mounting and collecting data on the crystal of {[N_3N_F]W(CN-t-Bu)$_3$}BPh$_4$, Jonathan Goodman for help in solving the structure of {[N_3N_F]W($CO)_2$}Na(ether)$_3$, and Jane Brock for helpful discussions. We also thank the National Science Foundation for funds to help purchase a departmental Bruker SMART/CCD diffractometer.

Supporting Information Available: Tables of crystal data and structure refinement, atomic coordinates, bond lengths and angles, anisotropic displacement parameters, and torsion angles for [N_3N]Mo(CN), {[N_3N_F]W($CO)_2$}Na(ether)$_3$, [N_3N_F]W(CO)V(Mes)$_3$, [N_3N_F]W(CN-t-Bu), and {[N_3N_F]W(CN-t-Bu)$_3$}BPh$_4$. This material is available free of charge via the Internet at http://pubs.acs.org.

OM990748U